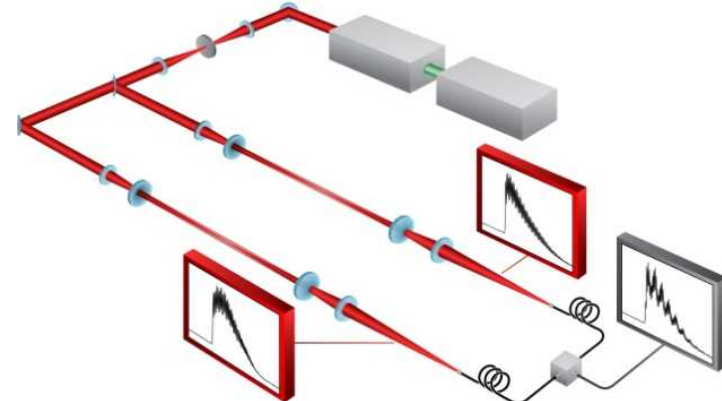
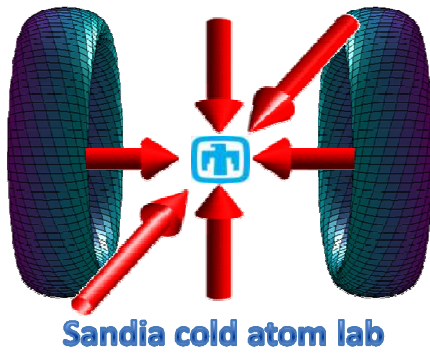


# Laser based techniques for nuclear forensics

SAND2012-5271P

*Laser based techniques for  
quantitative assessment of gas  
phase atoms and molecules*



# Outline

## ***Brief overview on nuclear forensics***

Importance

Dealing with short and long lived isotopes

## ***Comprehensive Test Ban Treaty***

The importance of Noble gasses

Detecting Noble gasses

Direct counting with light

## ***Basics of atomic and molecular spectroscopy***

Laser interactions with matter

The isotope shifts

## ***Advanced laser based techniques for remote detection***

Direct spectroscopic measurements

Optical isotope counting

new techniques for counting with frikin' lasers

# Nuclear Forensics is the next generation of nuclear deterrence

“Kim must be convinced that American nuclear forensics will be able to identify the molecular fingerprint of nuclear material from his Yongbyon Reactor. He must feel in his gut the threat that [if a detonated nuclear weapon is linked back to North Korea]. ... the United States will retaliate...”

*-Graham Allison, Washington Post, Oct 27 2006*



IAEA defines nuclear forensics as the analysis of intercepted illicit nuclear or radioactive material and any associated material to provide evidence for nuclear attribution.

The goal is to quantitatively assess the amount of a target analyte in order to determine either the nature of an event or trace (fingerprint) illicit nuclear or radioactive material.

# The effectiveness of radio-chemical forensics depends on isotope lifetime.

In typical radio-chemical analysis, one wants an isotope that lives long compared to the sample preparation time but short enough that the measurement time is reasonable.

$$N(t) = N_0 \exp(-t/\tau)$$

$$\text{where } \tau = t_{\text{half}}/\ln(2)$$

For dilute measurements: sample size  $10^4$  atoms

Half-life of 30 seconds: 5  $10^3$  counts in 30 seconds and  $\sim$ 10 minutes to collect the other 5  $10^3$  counts.

With a half-life of 10.7 years (Kr-85) in 1 month of counting  $\sim$ 50 counts. That requires a background rate of  $< .069$  counts per hour.

What is the motivation for monitoring radionuclides in the atmosphere?

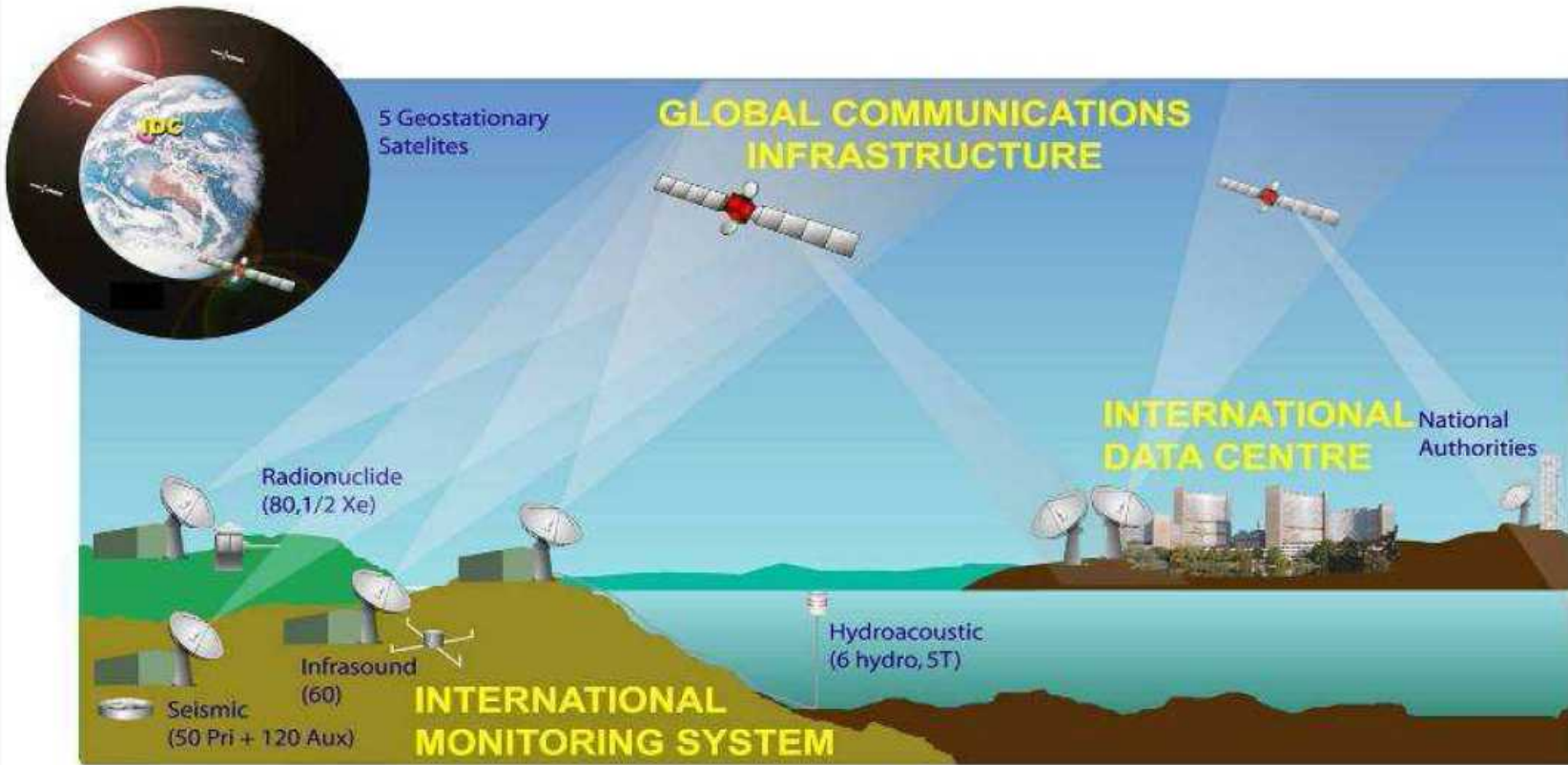
November 1, 1951 “Dog”



December 18, 1970 “Baneberry”

The comprehensive test ban treaty (CTBT) bans all nuclear testing.

CTBTA is creating an international monitoring system for detecting testing activities.

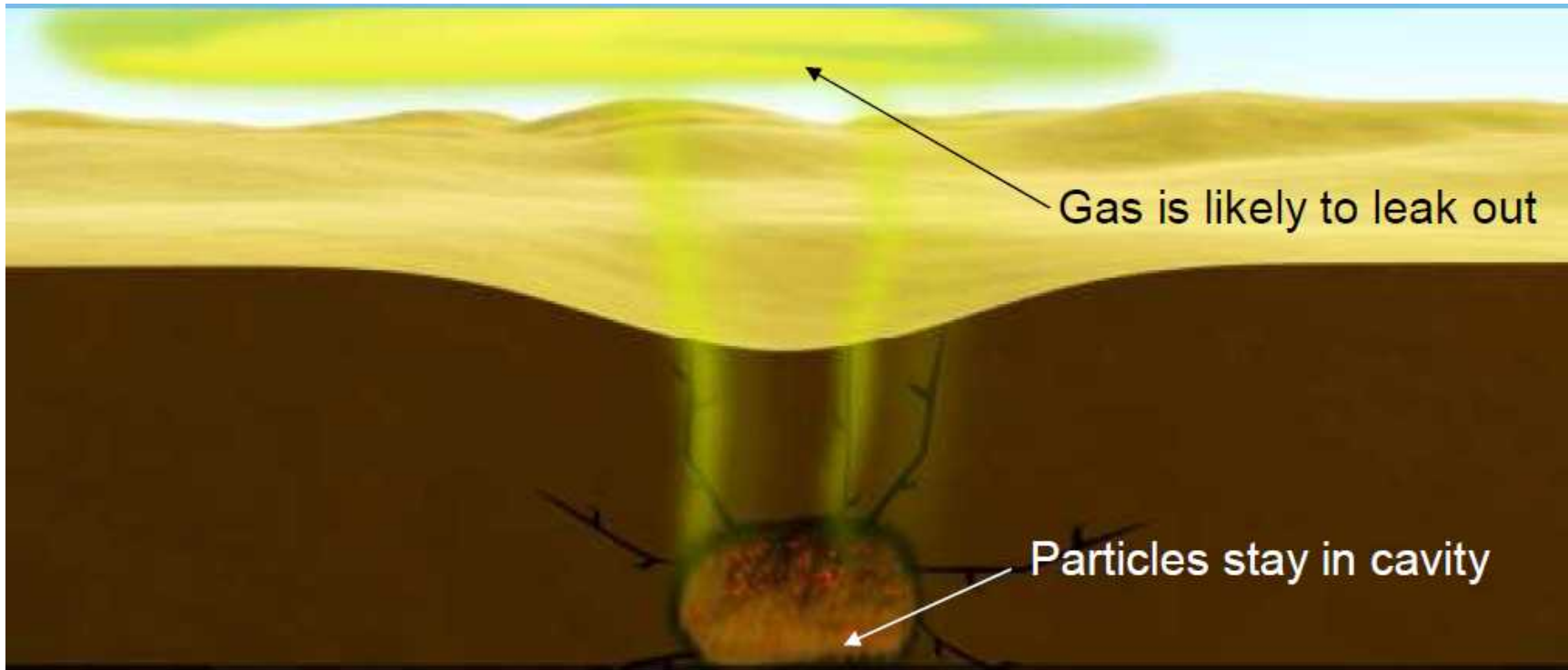


Taken from the SANUA project

In particular they are interested in atmospheric Xe concentrations, but all Noble gasses are of potential interest.

## Primary interest is in looking for Noble gasses.

Why Noble gasses?

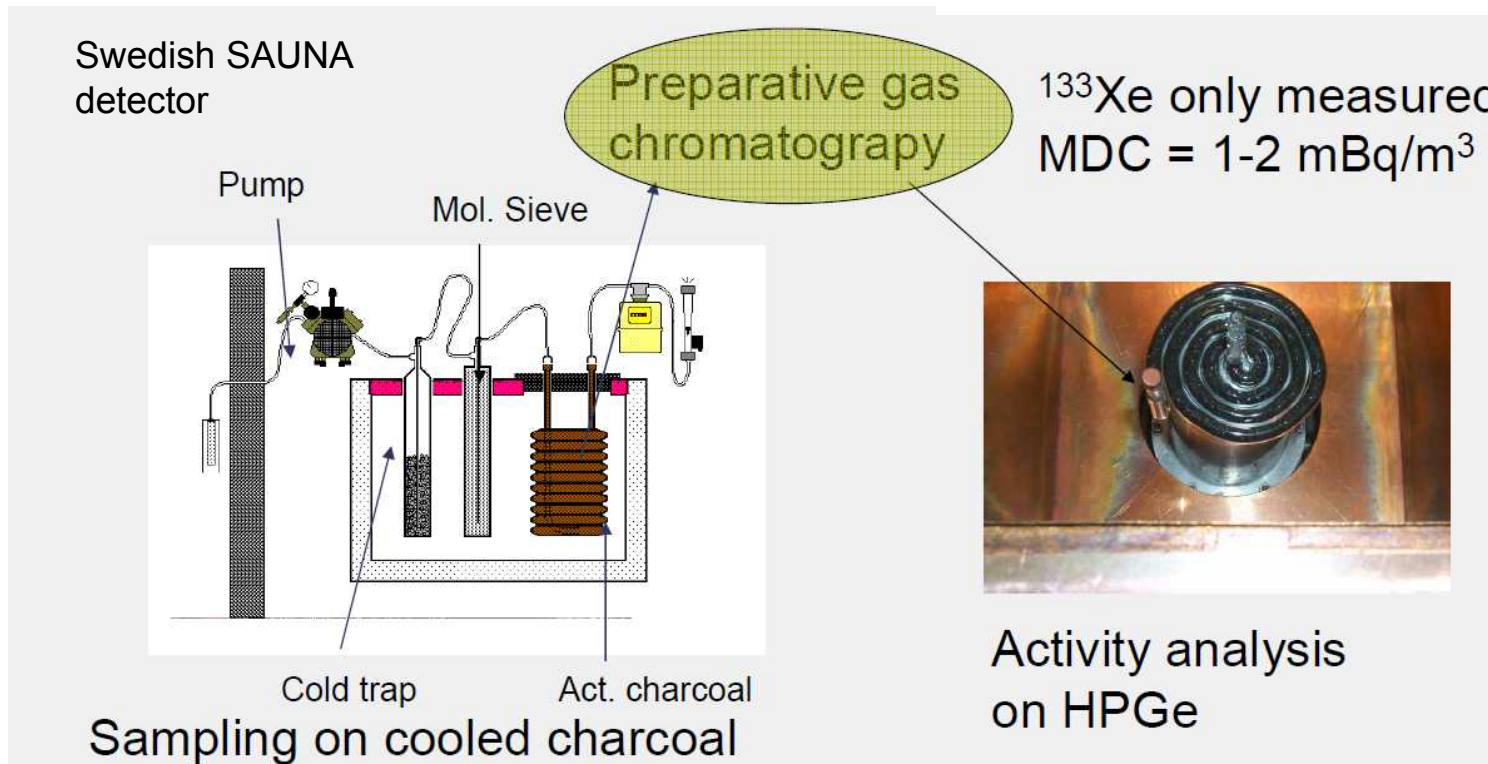
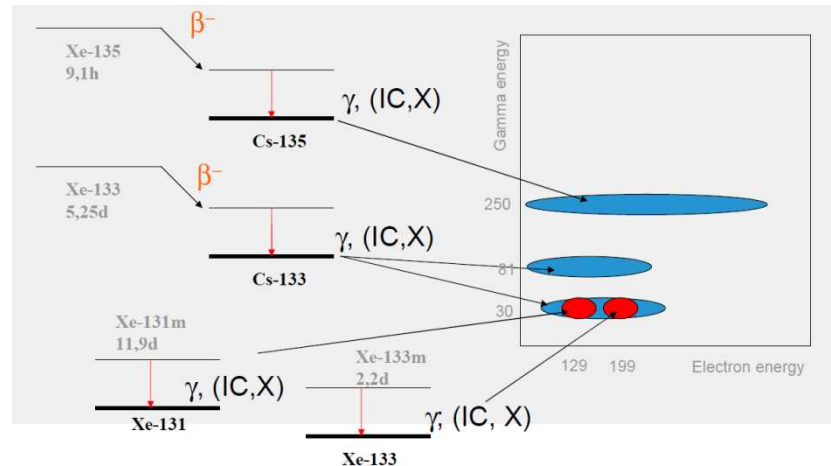


Simply put: Noble gasses are inert and hard to contain. They leak out through the soil. Other gas phase particles escape too, like Iodine, but the main interest is in Noble gases.

# How is radioactive Xe quantitatively measured

Gas is collected, filtered and processed and counted. The energy analysis is done by gamma ray counting.

Remote detection is ideal. Several counting based detectors are currently being tested by the CTBTA, Information is available from the CTBTA website:



## Importance of isotopic ratio-ing in source determination: the Xe example.

“Xenon isotopes are the most likely observable radioactive signature of underground nuclear explosions...”

“However, radioactive Xenon is released during normal operation of [civilian] nuclear facilities.”

“Nuclear reactor emission is never unambiguous, it can always be an aged explosion.”

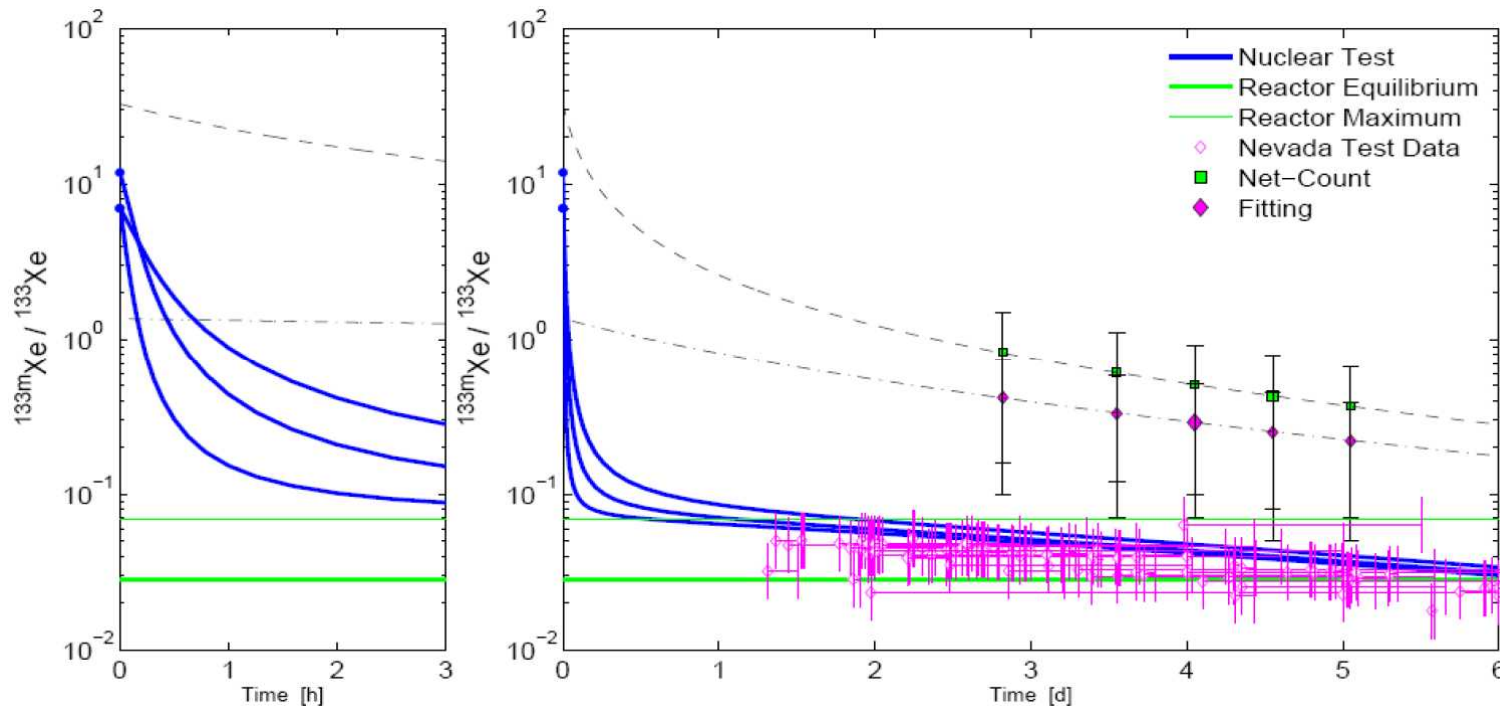
“Taking ratios of isotopes can greatly increase the confidence of the nature of the event.  $^{133}\text{mXe}/^{131}\text{mXe}$  and even better would include  $^{135}\text{Xe}$ .”

[http://esarda2.jrc.it/internal\\_activities/WC-MC/Web-Courses/01-Background/09-Environmental-Kalinowski.pdf](http://esarda2.jrc.it/internal_activities/WC-MC/Web-Courses/01-Background/09-Environmental-Kalinowski.pdf)

# Importance of isotopic ratio-ing in source determination: the Xe example.

“However, radioactive Xenon is released during normal operation of [civilian] nuclear facilities.”

“Nuclear reactor emission is never unambiguous, it can always be an aged explosion.”



[http://esarda2.jrc.it/internal\\_activities/WC-MC/Web-Courses/01-Background/09-Environmental-Kalinowski.pdf](http://esarda2.jrc.it/internal_activities/WC-MC/Web-Courses/01-Background/09-Environmental-Kalinowski.pdf)

## Why laser based detection?

Not all Noble gasses of interest have short lifetimes like Xe

Again: long-live isotopes are difficult to measure using decay based counting.

The detection of Kr-85 is widely viewed to be the best indicator of clandestine plutonium enrichment. –Karlsruhe report

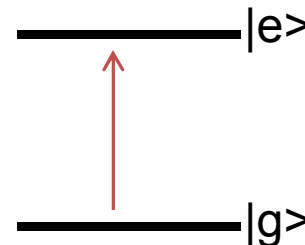
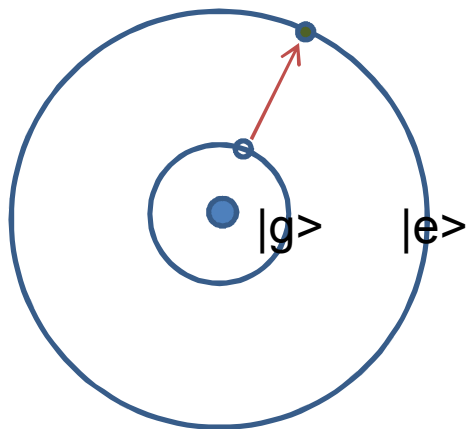
Kr is naturally abundant at 1ppm level and Kr-85 has a relative concentration is  $10^{-11}$ .

The half-live is 10.7 years. For rapid detection, massive amounts of gas must be sampled.

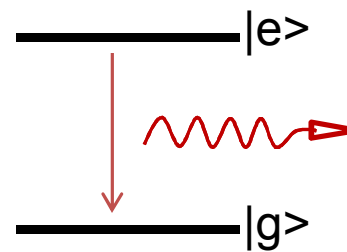
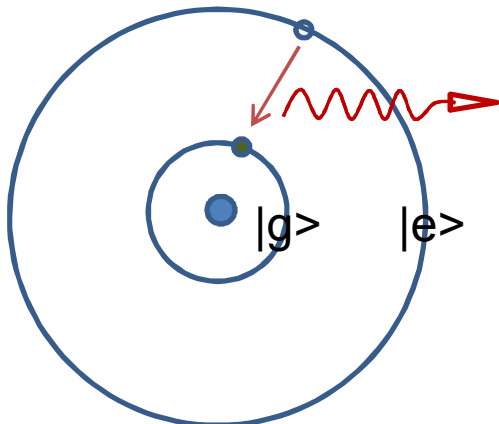
Spectroscopy give us a way to directly measure and quantify very dilute gas samples. Spectroscopy does not rely on measuring the decay products , but the directly measure the atom and the isotope.

# Light interacting with matter

Concept is that laser radiation moves electrons from the ground state to an electronically excited state.

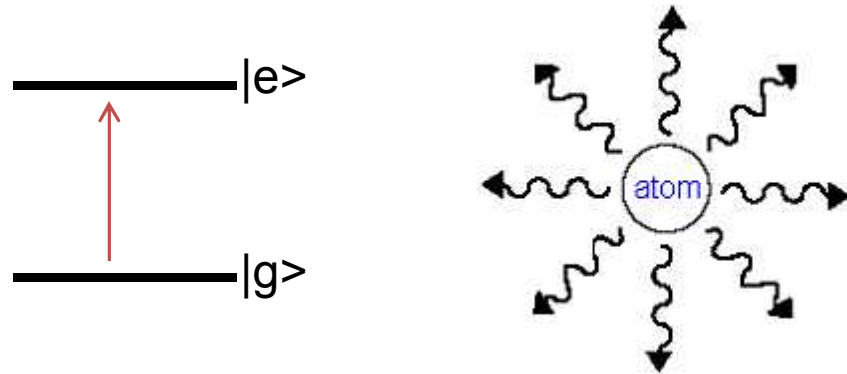


The excited state decays emitting a photon. Like a gamma particle emitted is a decay process the photon is emitted randomly.



## Two basic types of spectroscopy

### Fluorescence spectroscopy



An atom or molecule is excited by an incident light field, then spontaneously decays emitting a photon.

The atom scatters photons at a rate  $R_{sc}$  given by: 
$$R_{sc} = \left(\frac{\Gamma}{2}\right) \frac{(I/I_{sat})}{1 + 4(\Delta/\Gamma)^2 + (I/I_{sat})}$$

Where  $\Delta$  is the detuning and  $\Gamma$  is the lifetime of the excited state.

The spontaneous photon emission rate is given by  $\Gamma$ . This lifetime ( $1/\Gamma$ ) is on the order of 30-50ns. Unlike in beta/gamma decay, an atom can undergo multiple (thousands or more) absorption/emission cycles.

**A single atom can give thousands to millions of counts per second**

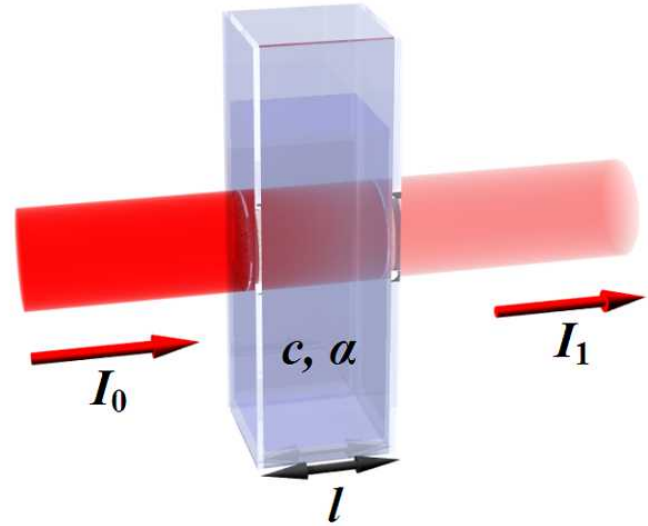
## Two basic types of spectroscopy

### Absorption spectroscopy

Instead of observing the spontaneously scattered photons one can look at the photon loss from the laser beam from absorption.

#### Beer's Law

$$T_{\text{transmission}} = I/I_0 = \exp(-\alpha l)$$

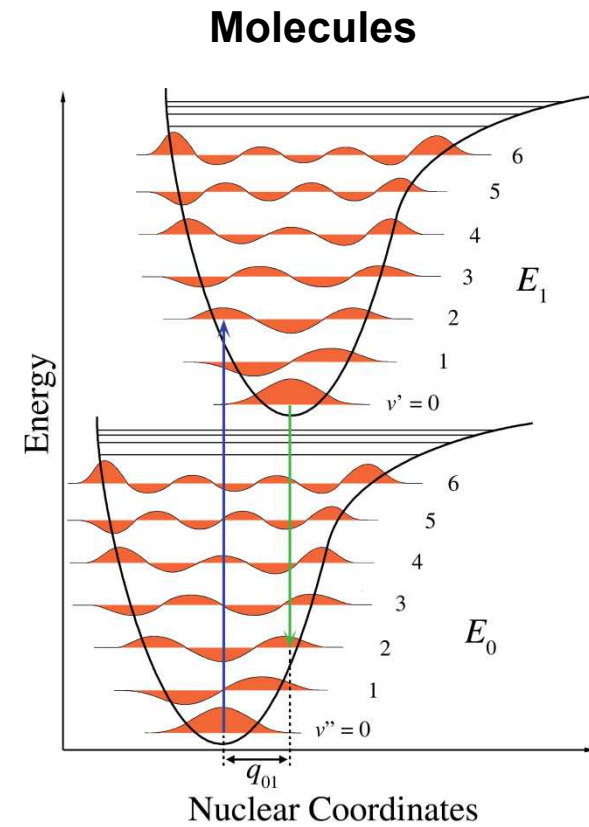
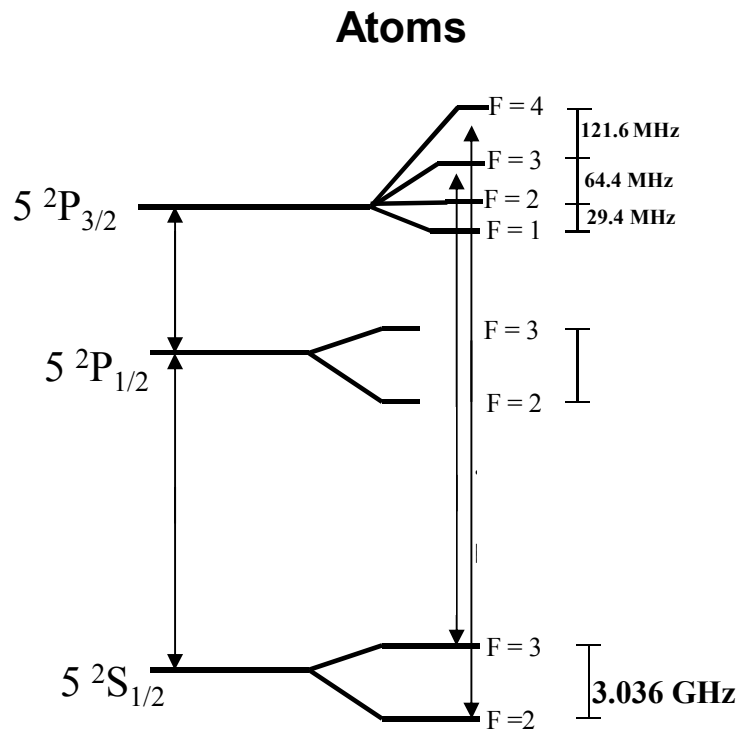


Where  $\alpha$  is the absorption constant .

Absorption is less sensitive than fluorescence as it is not background free (looking for loss of light). Absorption is however more quantitative since all the beam can be collected.

Differences between atoms and molecules come down to quantum mechanical selection rules.

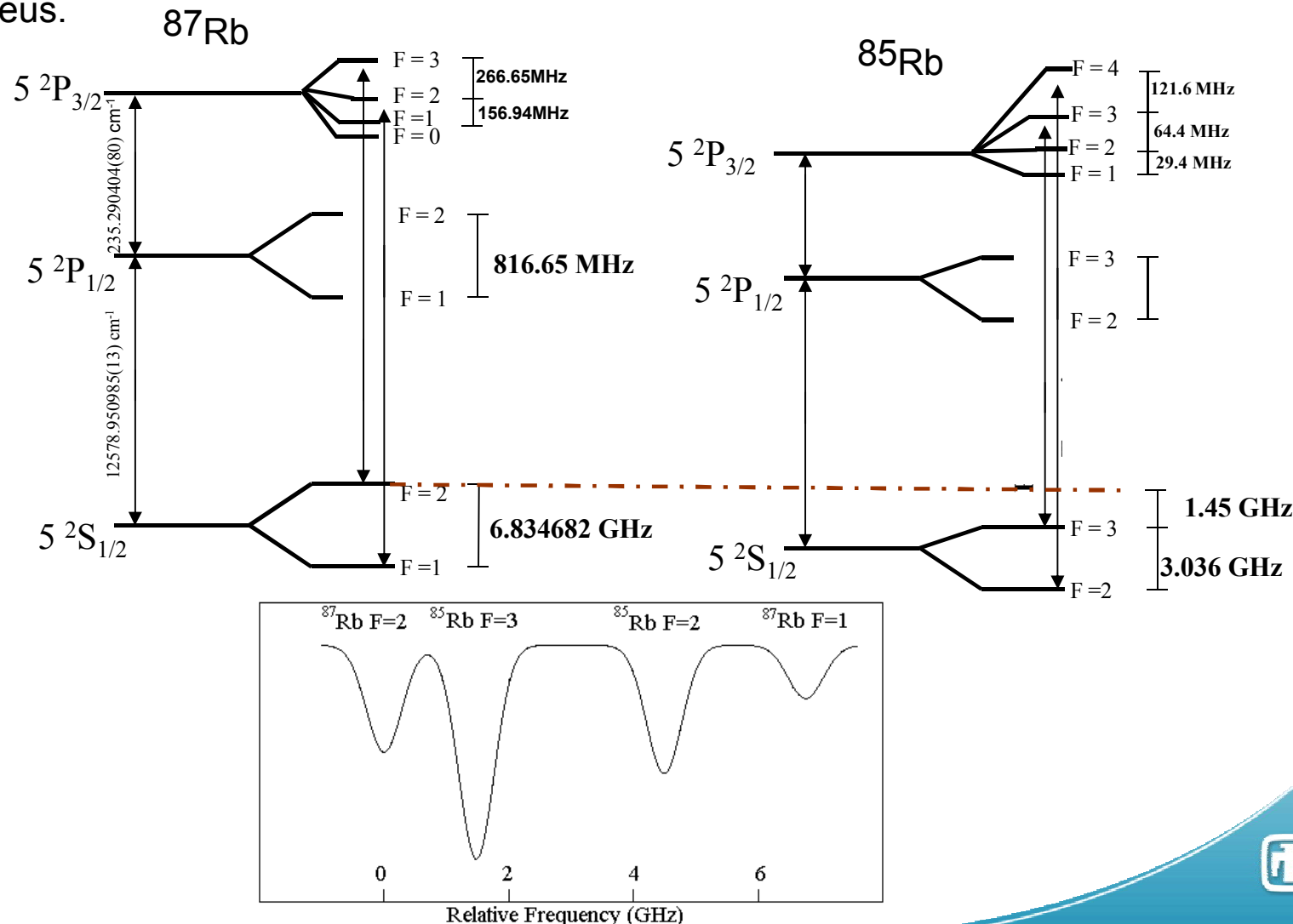
For optical electronic transitions atoms have simple  $\Delta F = +/-1, 0$  selection rule. Molecules have vibrational levels and their transition are governed by Franck-Condon principle that the excited state decays to the ground vibrational level that has the most overlap with the electronic wave function.



Molecules are much harder to detect as one gets fewer scatters per atom.

The isotope shift gives each atomic and molecular isotope a unique set of optical frequencies.

The origin of the isotope shift is from both the shift in the center of gravity and distortions of the electronic orbital from the addition or subtraction of neutrons in the nucleus.



*The impact of the isotope shift is the ability to discriminate between isotopes based on one or more optical transitions*

*The photon scattering rate  $R_{sc}$*

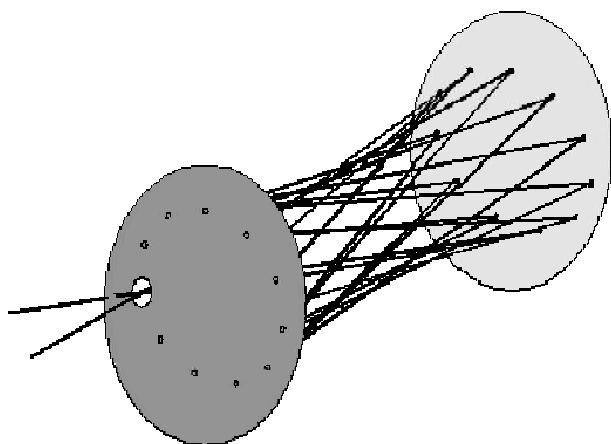
$$R_{sc} = \left( \frac{\Gamma}{2} \right) \frac{(I/I_{sat})}{1 + 4(\Delta/\Gamma)^2 + (I/I_{sat})}$$

With a detuning of 1.45 GHz and a natural line width ( $\Gamma$ ) of 5MHz, the detuning scales as  $(4(\Delta/\Gamma)^2)^{-1}$ .

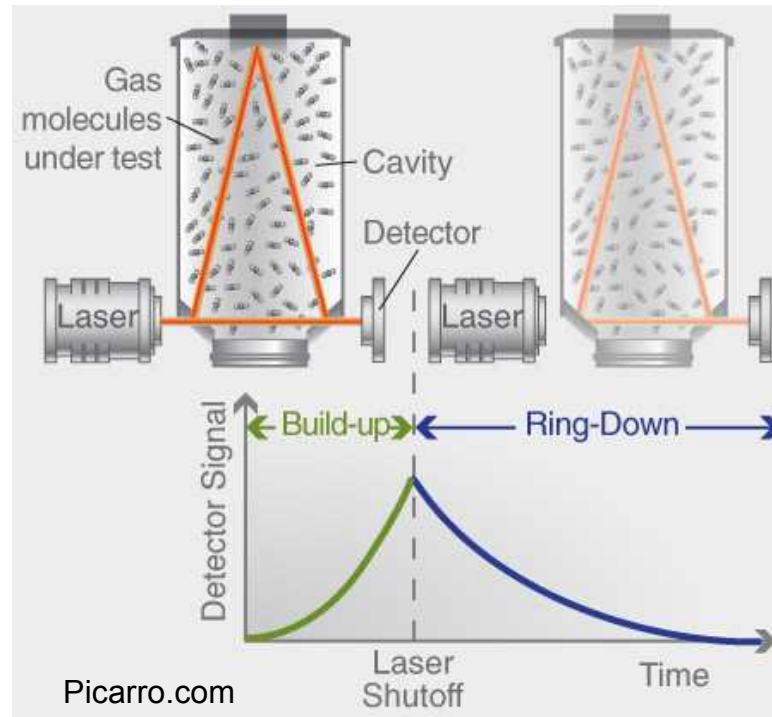
That is a factor of  $3 \times 10^5$  discrimination between the two Rubidium isotopes.

We can optically discriminate between isotopes and the measurement is not effected by the lifetime of the isotope, but (to first order) the laser parameter .

Sensitivity of absorption is proportional to the absorption cross-section and the path length.



Multi-pass cells



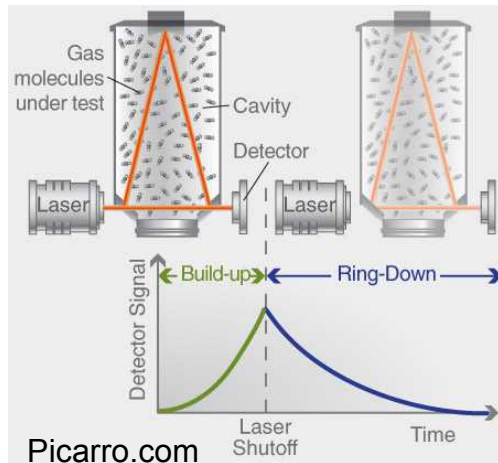
Cavity-ring-down

The cross-section is set by the analyte. But the path length,  $dx$ , can be adjusted to maximize weak absorptions.

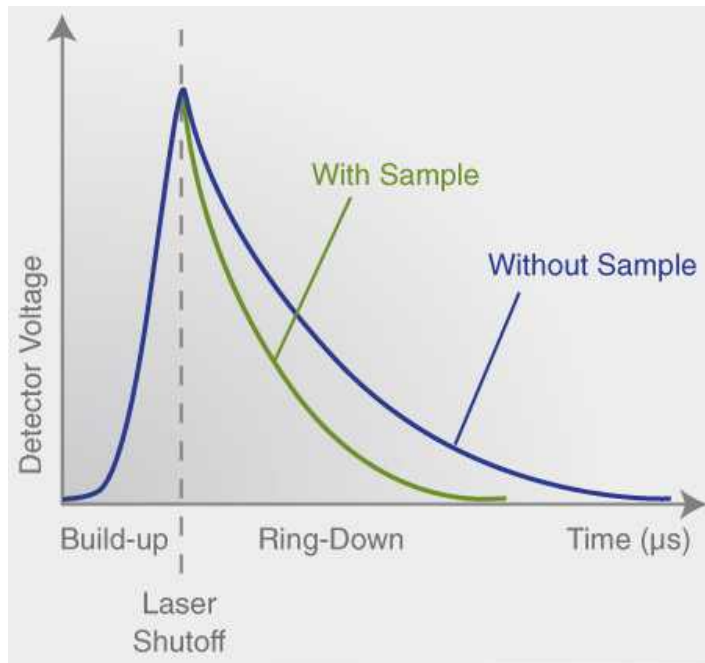
The trick with absorption spectroscopy is to have as long of a path length ( $dx$ ) as possible. These techniques have been in development for over 30 years.

For atmospheric spectroscopy several companies like Picarro and Los Gatos (both in the south bay) sell devices for remote monitoring of  $\text{CO}_2$ ,  $\text{NO}_x$   $\text{NH}_3$  ...

For high sensitivity the measurements can take hours but are typically on the order of 60 seconds for high concentration gasses and 30 minutes for low concentration gasses.



Typical experimental setup is based on cavity ring-down spectroscopy where light is coupled to an optical cavity and allowed to ring-down. The laser is typically a narrow band diode or Quantum-Cascade laser QCL.



The ring-down of the light in the cavity is modified by the sample.

The intensity  $I(t)$  is given by:

$$I(t) = I_0 \exp(-t(\frac{1}{\tau} + \alpha c))$$

The  $(\alpha c t)$  term is just Beer's law where  $(c t)$  is the path length the light travels in the cavity.

With good optics this length can be Km in a 50cm sample size.

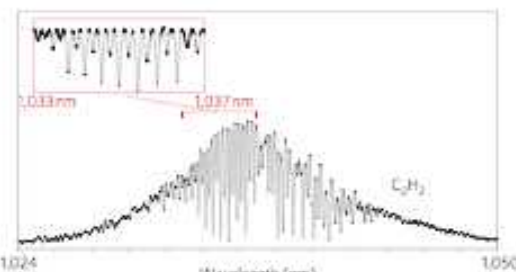
The one draw back is that the high finesse cavity only looks at a narrow frequency range  $\sim 10$  kHz.

To address this techniques have been developed to use fs-lasers with broad bandwidths, coupled to optical cavities. Known as fs-frequency-comb spectroscopy.

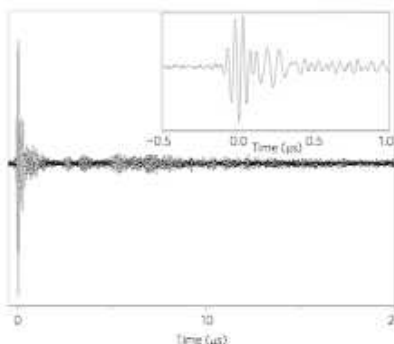


## Cavity-enhanced dual-comb spectroscopy

Birgitta Bernhardt<sup>1</sup>, Akira Ozawa<sup>1</sup>, Patrick Jacquet<sup>2</sup>, Marion Jacquet<sup>2</sup>, Yohei Kobayashi<sup>3</sup>, Thomas Udem<sup>1</sup>, Ronald Holzwarth<sup>1,4</sup>, Guy Guelachvili<sup>2</sup>, Theodor W. Hänsch<sup>1,5</sup> and Nathalie Picqué<sup>1,2\*</sup>

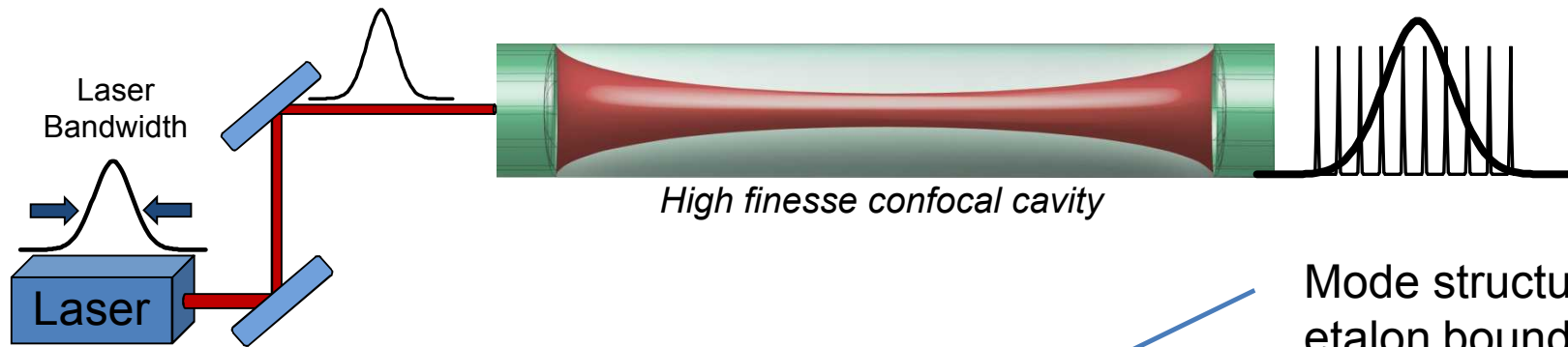


**Figure 3 | Cavity-enhanced FC-FTS spectrum of  $\text{C}_2\text{H}_2$ .** The overtone bands of  $\text{C}_2\text{H}_2$ , recorded according to the cavity-enhanced FC-FTS principle. Illustrated in Fig. 1, are plotted with a linear intensity scale. The high-finesse cavity is filled with 3 hPa of  $\text{C}_2\text{H}_2$  in natural abundance. The laser spectrum extends from 1,025 to 1,050 nm. The absorption spectrum reports the  $\text{C}_2\text{H}_2$  intensity alternation of the  $3\nu_3$  vibrational band centred at 1,037.4 nm. The inset shows signatures around 1,035 nm belonging to the R-branch (from R(19) to R(1)).

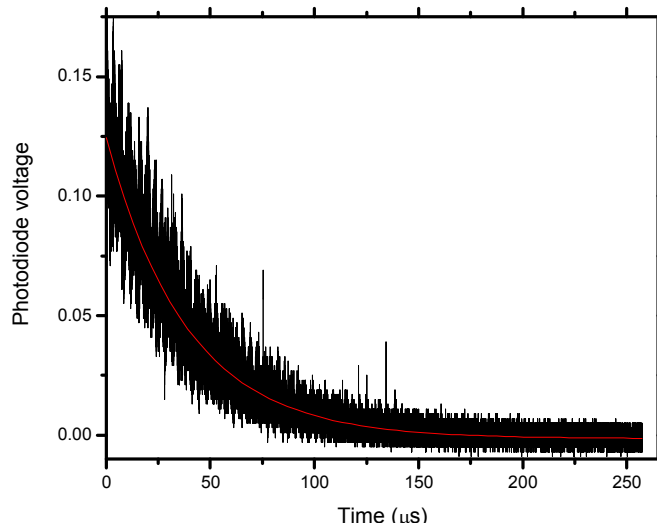


**Figure 2 | Time-domain interferogram.** Interferogram of  $\text{C}_2\text{H}_2$  acquired within 20  $\mu\text{s}$ , without averaging. This unweighted interferogram leads to a spectrum with 4.5 GHz unapodized resolution. When an interferogram is unweighted, the shape of the spectral line is the convolution of the true spectrum and a sinc function (that is, the Fourier transform of the boxcar finite-measurement time truncation function). If a well-chosen weighting numerical function was adopted, the true spectrum would be convolved with the Fourier transform of this function. This operation is called apodization, as it considerably reduces the amplitude of the sidelobes of the convolving function at the expense of a loss in resolution. The interferogram repeats itself with a period that is the inverse of the difference in the repetition frequencies of the two combs. The burst, arbitrarily set at 0  $\mu\text{s}$ , corresponds to the overlap of two femtosecond pulses. The inset shows an enlarged view of the burst area. Other than the burst, that is, for times longer than 1  $\mu\text{s}$ , the interferometric signal exhibits the typical modulation due to the molecular lines. It only occurs on one side of the burst, as the absorbing sample held in the high-finesse resonator interacts with only one of the two combs.

While exceeding sensitive it requires 2 stabilized frequency comb lasers and only works at a few frequencies. Not general enough (yet) for security applications.

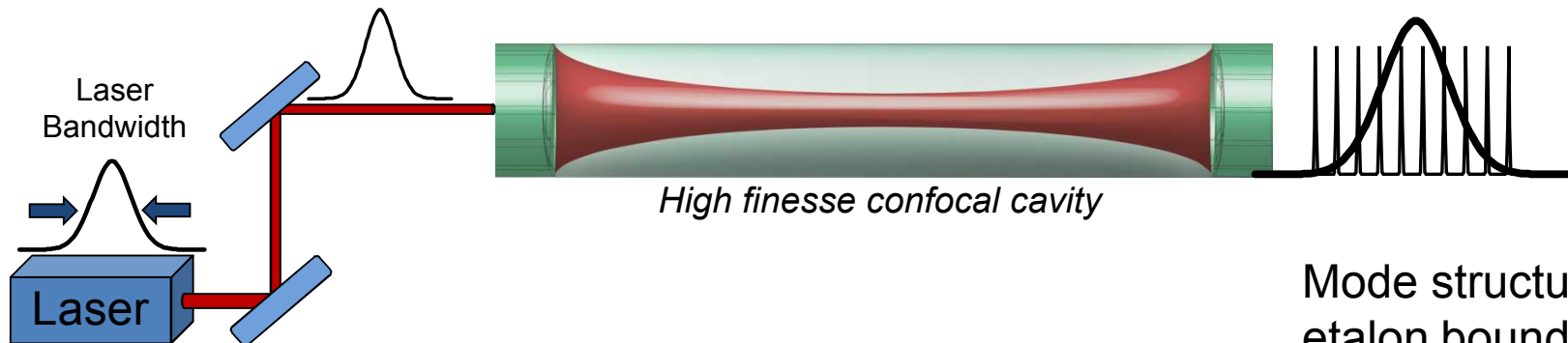
*Broad band lasers and cavity ring-down*

Mode beating on the detector adds noise to the ring-down signal



Modes beat at the free-spectral range (or cavity spacing) of the etalon.

### *The mode beating problem*



Solution?

Get rid of the mode structure.

Volume 217, number 1,2

CHEMICAL PHYSICS LETTERS

7 January 1994

### Coherent cavity ring down spectroscopy

Gerard Meijer, Maarten G.H. Boogaarts, Rienk T. Jongma, David H. Parker  
*Department of Molecular and Laser Physics, University of Nijmegen, Toernooiveld, 6525 ED Nijmegen, The Netherlands*

and

Alec M. Wodtke<sup>1</sup>  
*Department of Chemistry, University of California, Santa Barbara, CA 93106, USA*

Received 29 October 1993

In a cavity ring down experiment the multi-mode structure of a short resonant cavity has been explicitly manipulated to allow a high spectral resolution, which is advantageous for the overall detection sensitivity as well. Coherent cavity ring down spectroscopy is performed around 298 nm on OH in a flame.

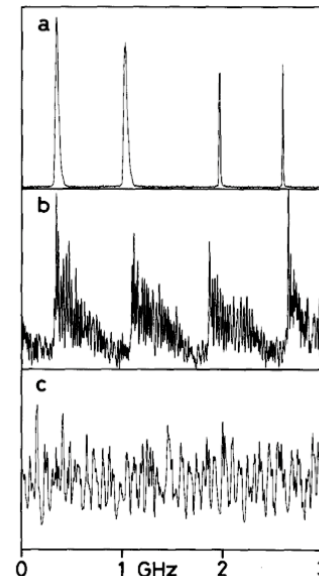
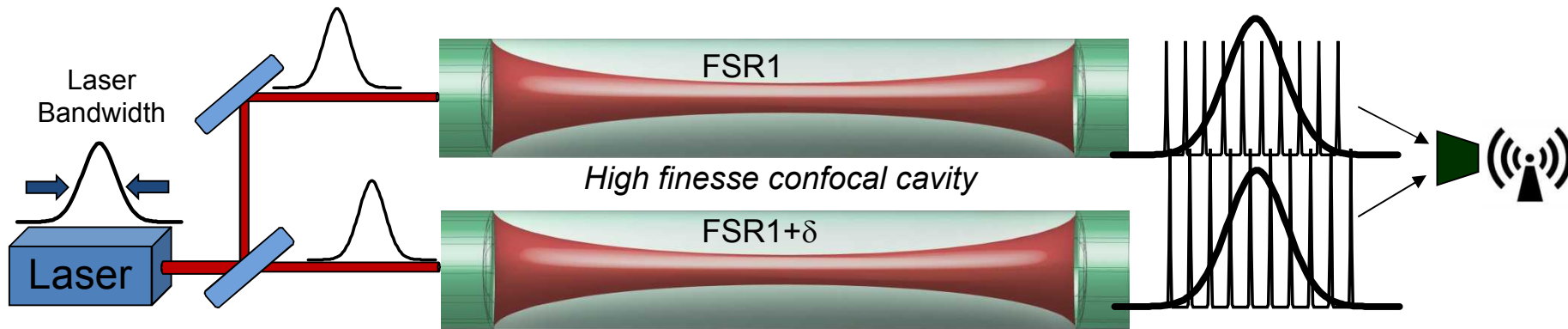


Fig. 1. Mode-spectrum of the ring down cavity for three different mirror separations  $d$ : (a)  $d=10.0$  cm; (b)  $d=10.2$  cm; (c)  $d=11.5$  cm. A rapid congestion of the spectrum is seen when the cavity is detuned from confocal. The spectra are measured by monitoring the transmission of the cavity while a narrowband ( $\leq 5$  MHz) cw UV laser is scanned over 3 GHz (6 GHz/min scan-rate) around 318 nm.

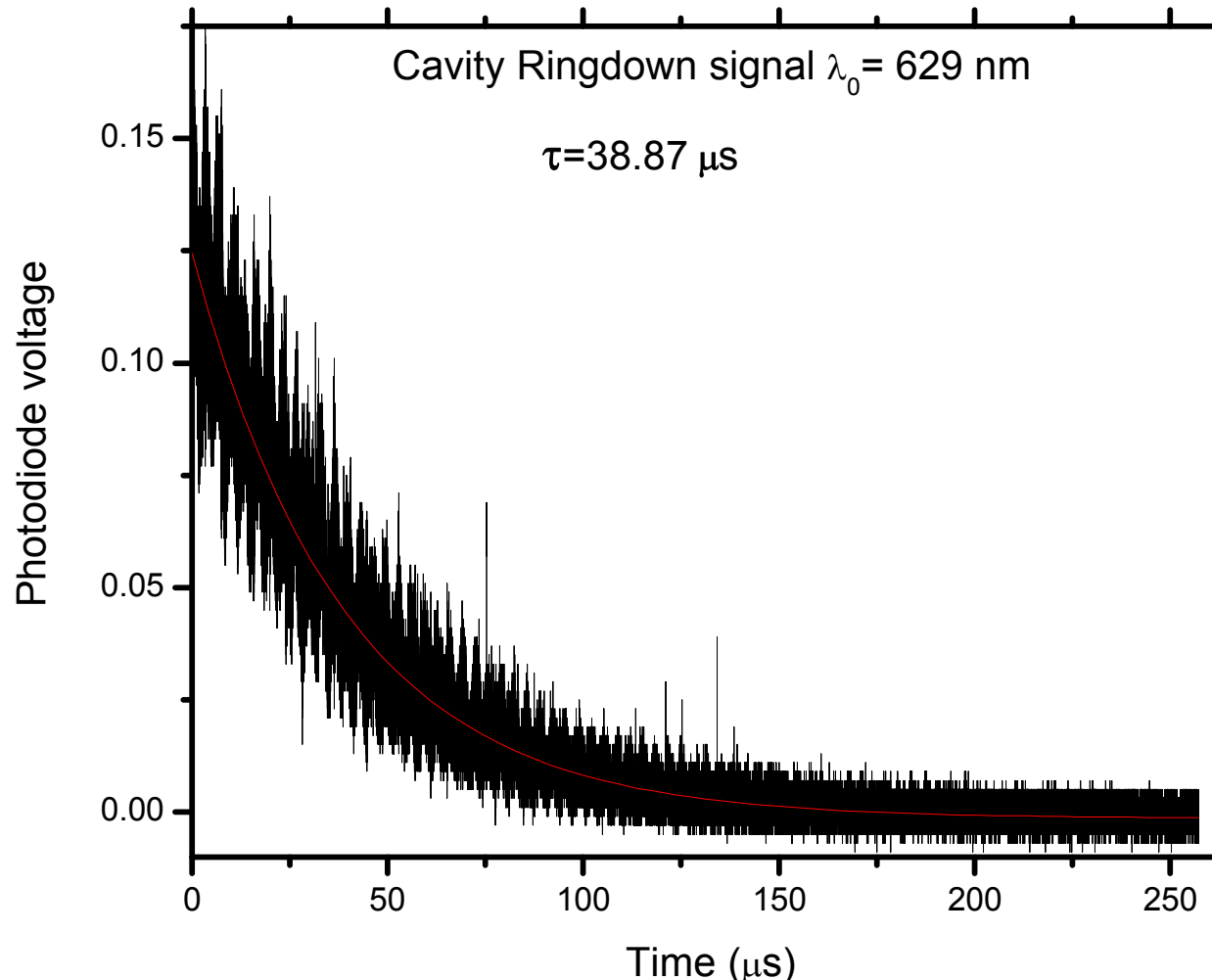
*dual etalon cavity ring-down spectroscopy**Make use of the cavity mode structure*

Add a second cavity, with a slightly different free-spectral range and overlap the output of both cavities onto a single photo-detector.

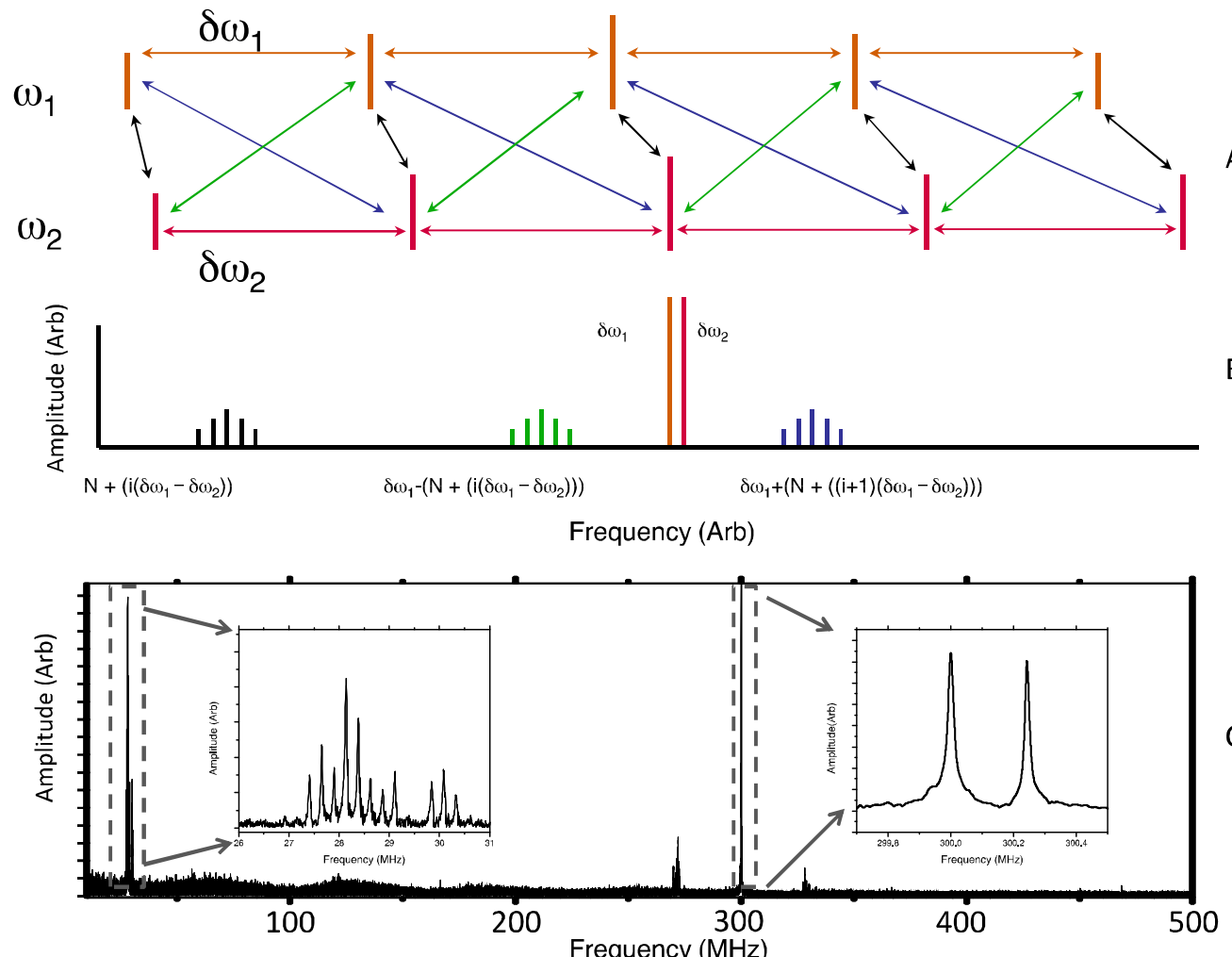
The different frequency modes will interfere. The heterodyne signal of each nearest-neighbor frequency pair will have a unique radio-frequency. This allows us to extract high resolution spectra from under the bandwidth of a single broadband laser pulse.

*Standard cavity ring-down signal but with mode beating*

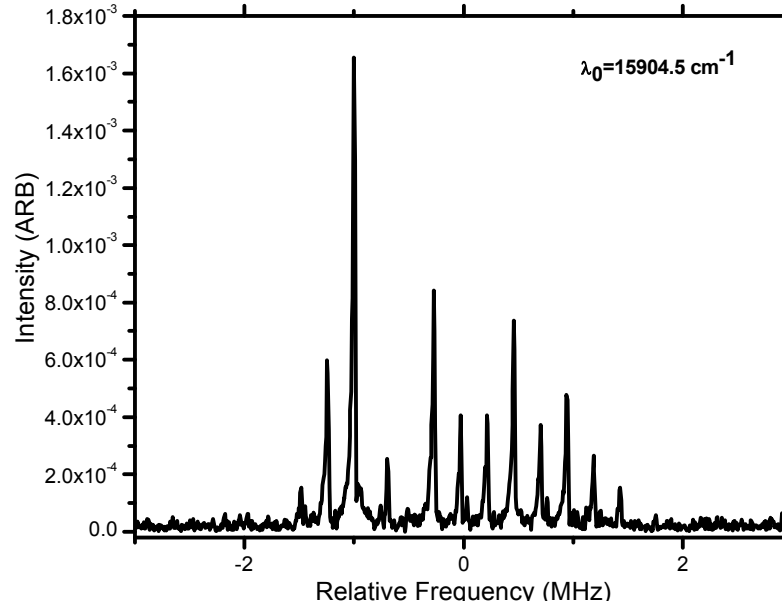
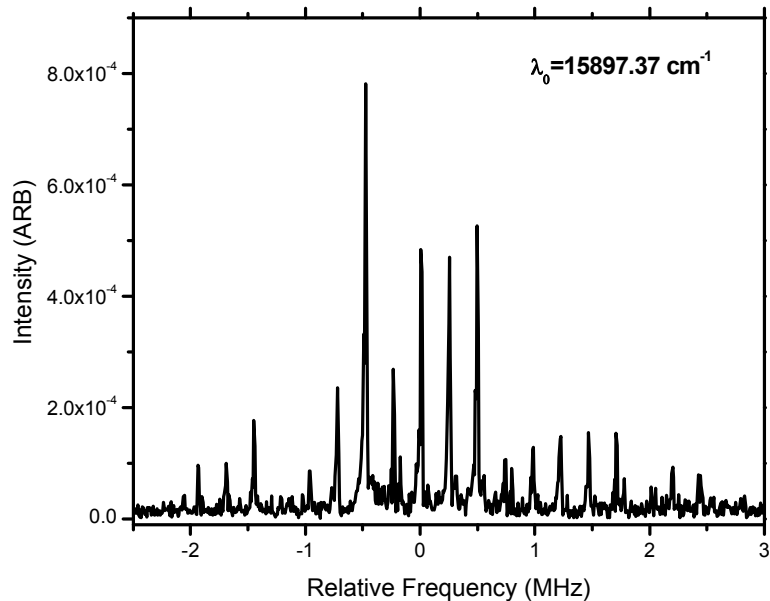
Single laser shot data:



*The Fourier transform of the cavity ring-down signal reveals the frequencies*



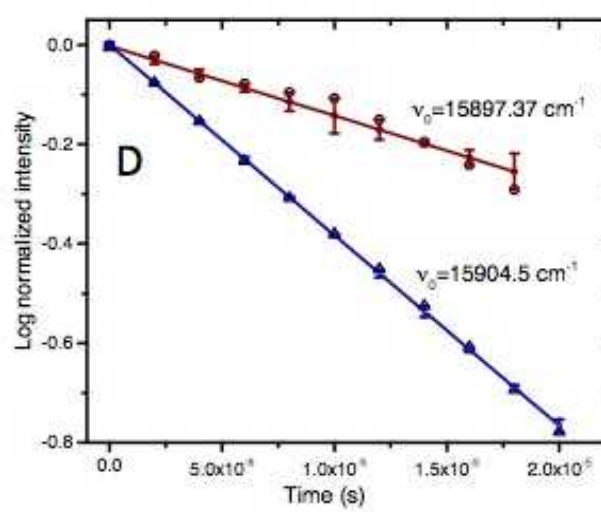
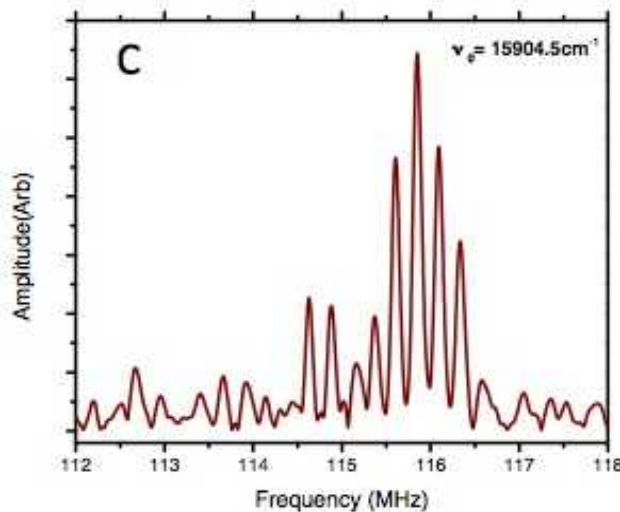
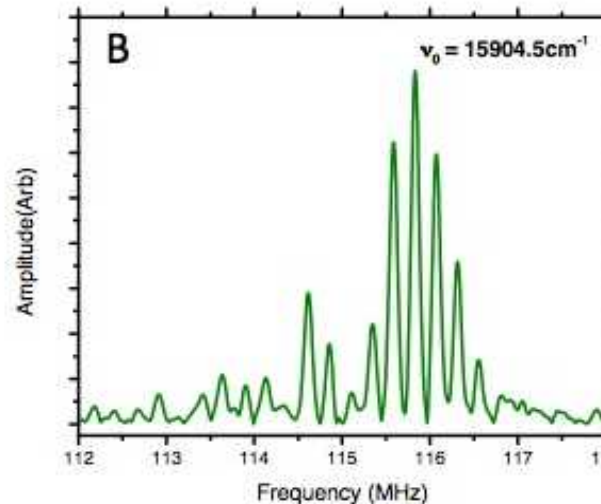
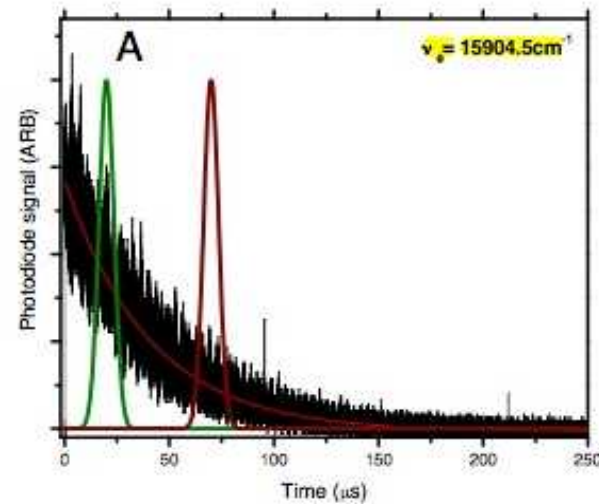
*However, a non-transform limited laser has phase/frequency structure*



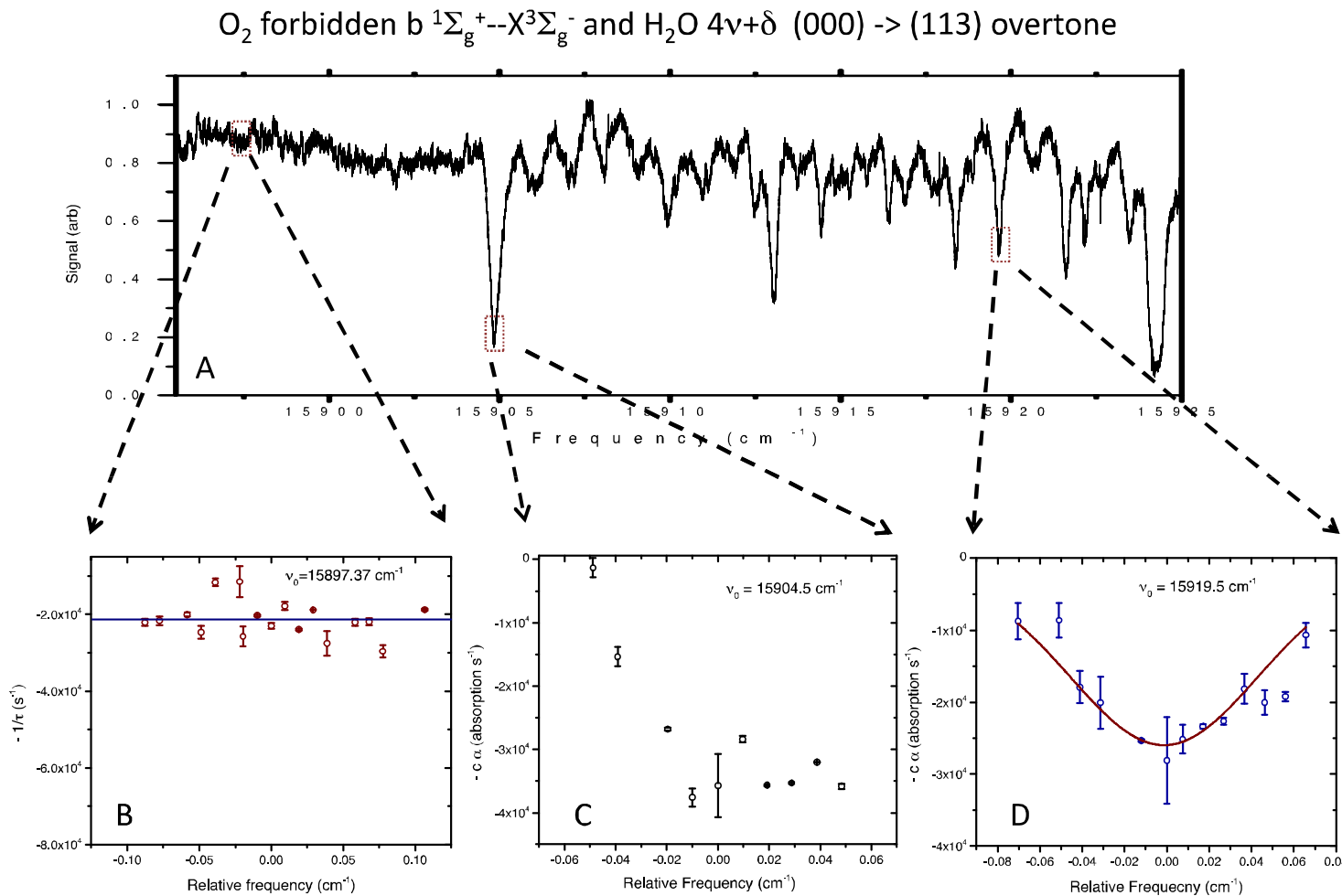
Each laser shot has different mode structure under the bandwidth of the laser.

This makes direct extraction of the spectrum impossible.

*The FT can be done as a function of time giving the CRD signal for each frequency mode.*



## Extracted Broad band spectra.



We obtain, single shot spectrum. Each point has a width of 250kHz spaced by 300MHz over the laser bandwidth

Fluorescence measurements are inherently more sensitive, they do not require high path length, so why does anyone do absorption?

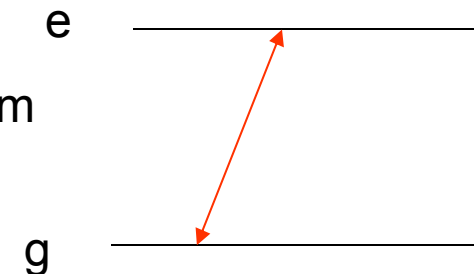
Fluorescence has two draw backs:

- 1) Scattered light must be collected, there is a built in detection in-efficiency that must be calibrated since we are no longer looking at an  $I/I_0$  difference.
- 2) The atoms are moving. I said before a single atom can give millions of photons per second, but under normal thermal conditions the atoms are moving at 300+ m/s . So a typical experimental setup only interrogates the atoms for  $\sim 100 \mu\text{s}$ . Less than 100 photons per atom are realized, making a single atom measurement hard to impossible.

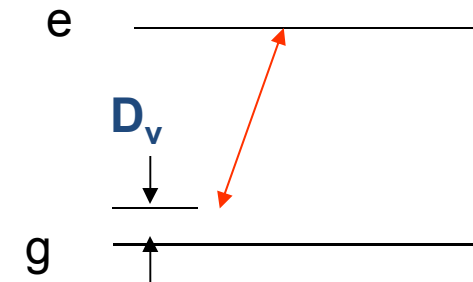
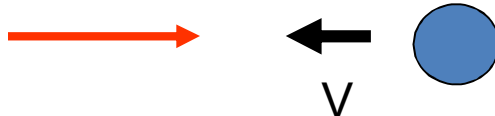
This is where laser cooling and atom trapping become effective. Atoms can be slowed to mm/s and observed to 10-s of seconds. Making single atom detection possible.

## Atom Trapping and Laser cooling

Rb

 $l = 780 \text{ nm}$  $t = 27 \text{ ns}$ 

Doppler shift can put laser into resonance

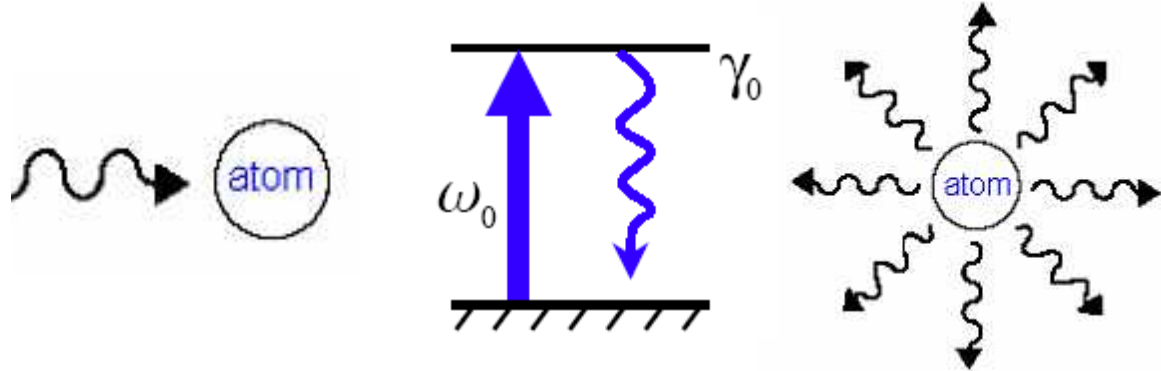


- Absorption gives 'kick' against 'v'
- Emission is random 'kick'

Net result of many absorptions is slowing

## Atom Trapping and Laser cooling:

Laser light can remove momentum from atoms by absorption and spontaneous emission.



$$F_{average} = \frac{\Delta_{momentum}}{\Delta_{time}} = \frac{1}{2} \hbar |\mathbf{k}| \gamma$$

This is the maximum average force assuming a saturated transition.

Doppler shift:

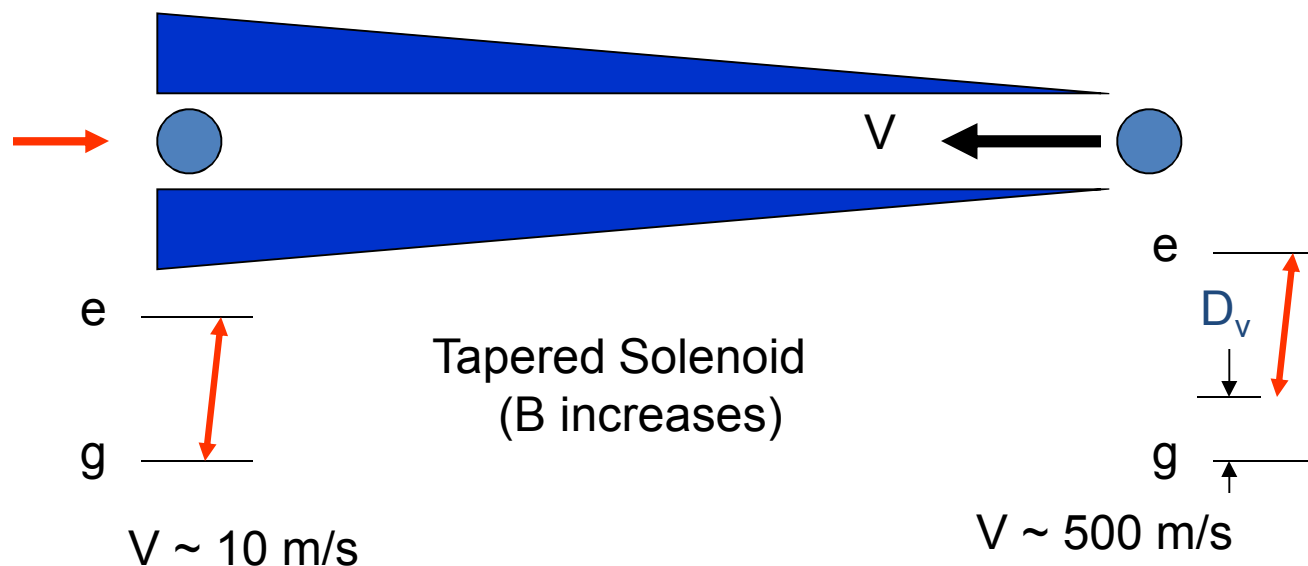
$$\nu = \nu_0 \frac{1 + \frac{V}{c}}{\sqrt{1 - \left(\frac{V}{c}\right)^2}},$$

For 100 m/s Rb the shift is 128MHz

For 1m/s Rb the shift is 1.3 MHz

Rb Linewidth  $\sim$  6MHz

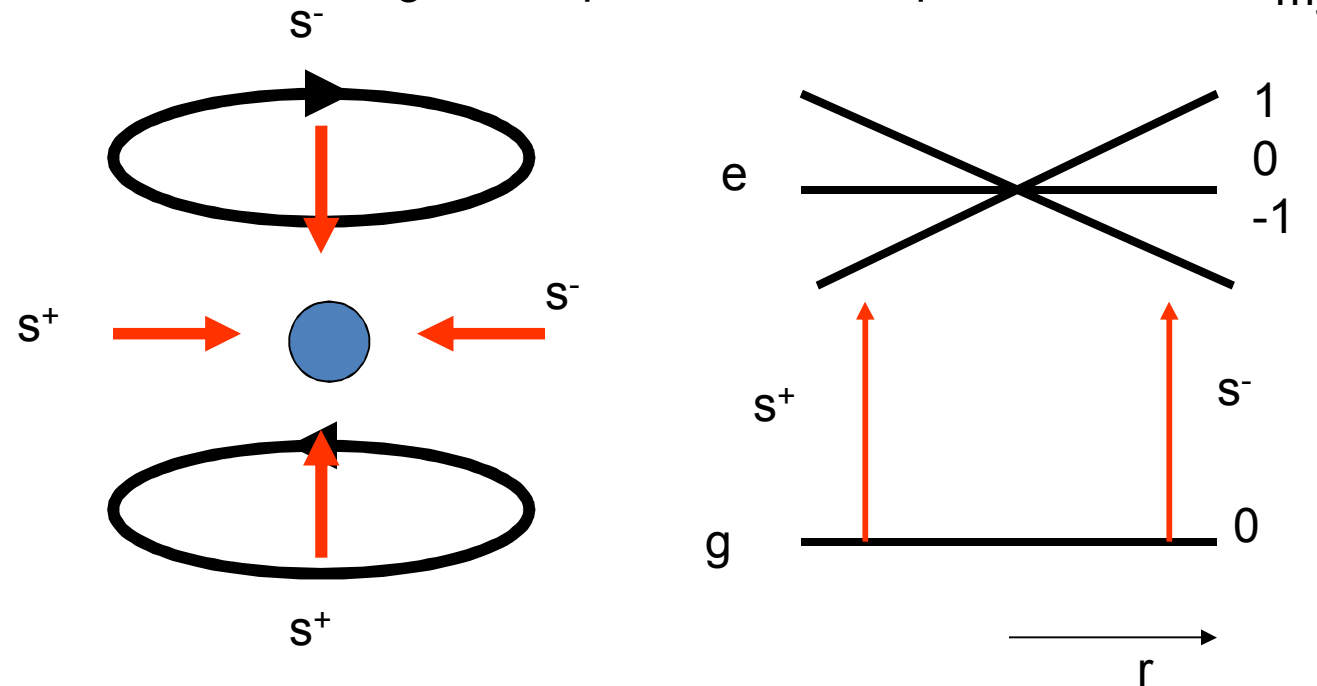
(W. Phillips): Zeeman Shift Change energy structure of atom during cooling

Zeeman Shift  $E \sim \mathbf{m} \times \mathbf{B}$ 

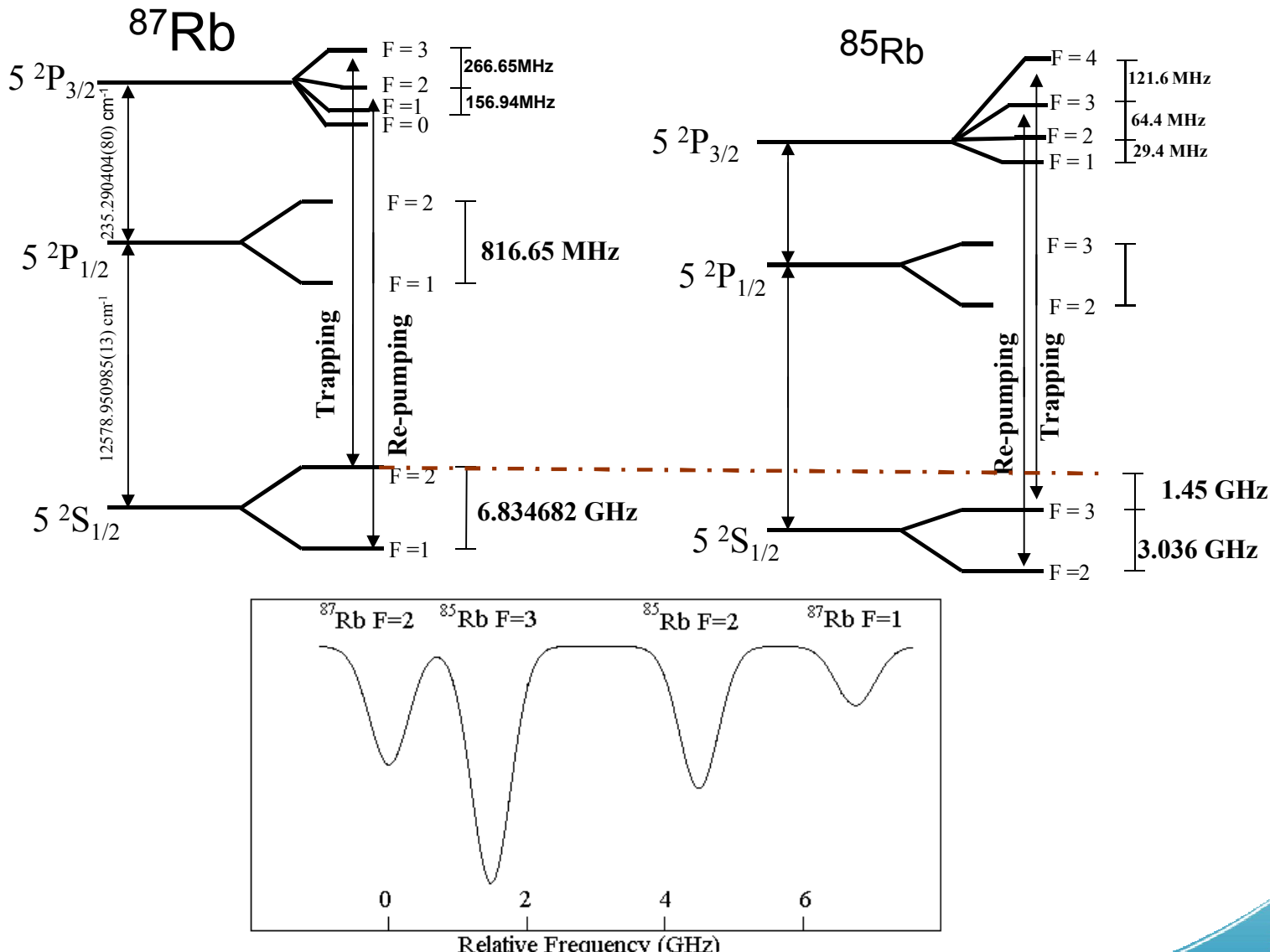
**Atom Trapping and Laser cooling:**

Atom velocities in a MOT are  $\sim$  few cm/s : no real Doppler Shift to provide directional or spatial confinement: “Optical Molasses”

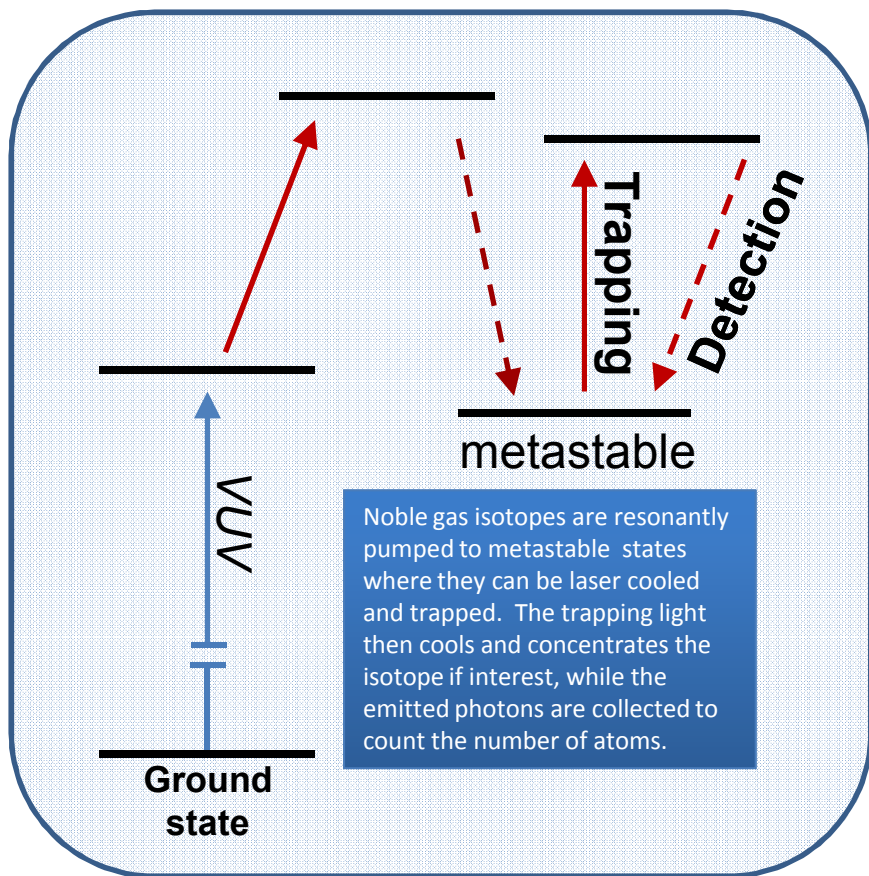
MOT: Spatial restoring force comes from the Zeeman shift. A magnetic field in anti-Helmholtz configuration provides the required field.



Limit:  $T_{\text{Doppler}} \sim 40 \text{ mK}$



All Noble gasses can be treated like other atoms once they are exited to a meta-stable state.



The Noble gasses have low energy excited states that only couple via two photons to the ground state. These long lived states are considered metastable.

The metastable state can be reached either by electron impact or optically (as shown)

The trapping and detection transition are built off the metastable state, such that the transition are in a region where laser light is easily generated.

Once the atoms are confined single atoms can be measured

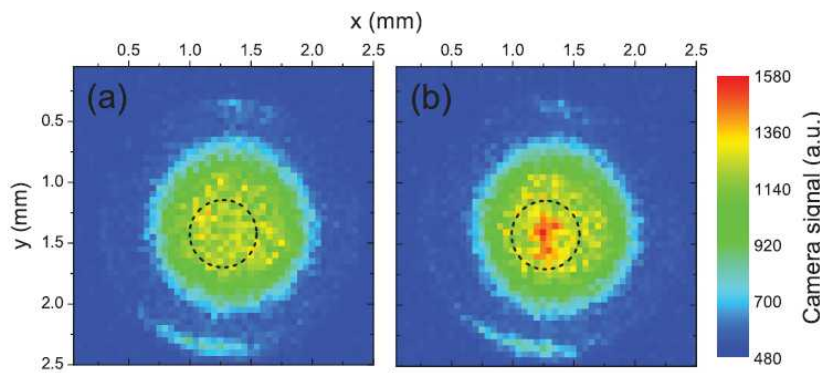


FIG. 2 (color). False-color CCD images of the MOT at  $^{39}\text{Ar}$  settings. In (a) no atom is present; the background is dominated by scattered laser light imaged through a 1 mm diameter aperture and an additional ring-shaped diffraction pattern. In (b) the fluorescence emitted by a single  $^{39}\text{Ar}$  atom can be clearly distinguished above background. The dashed circle indicates a 0.5 mm diameter region of interest for averaging the CCD signal.

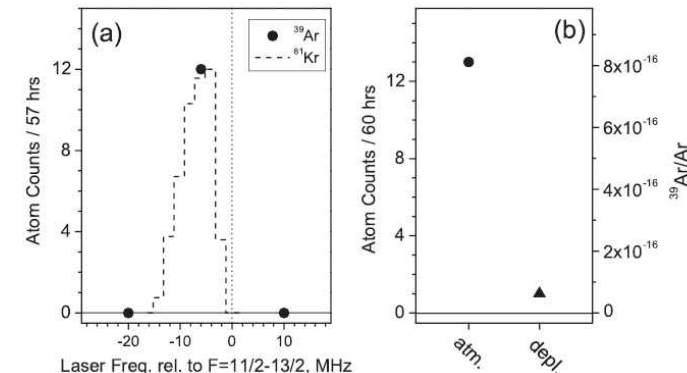
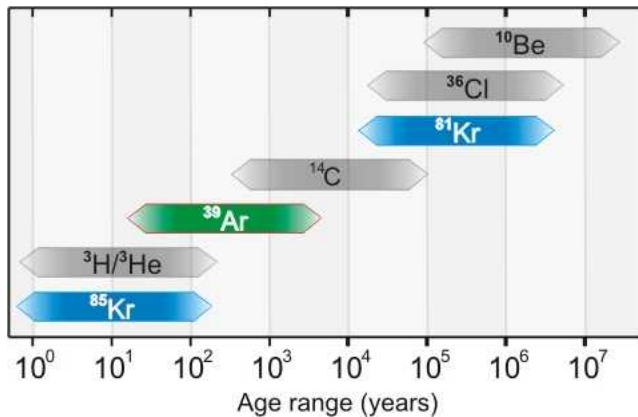
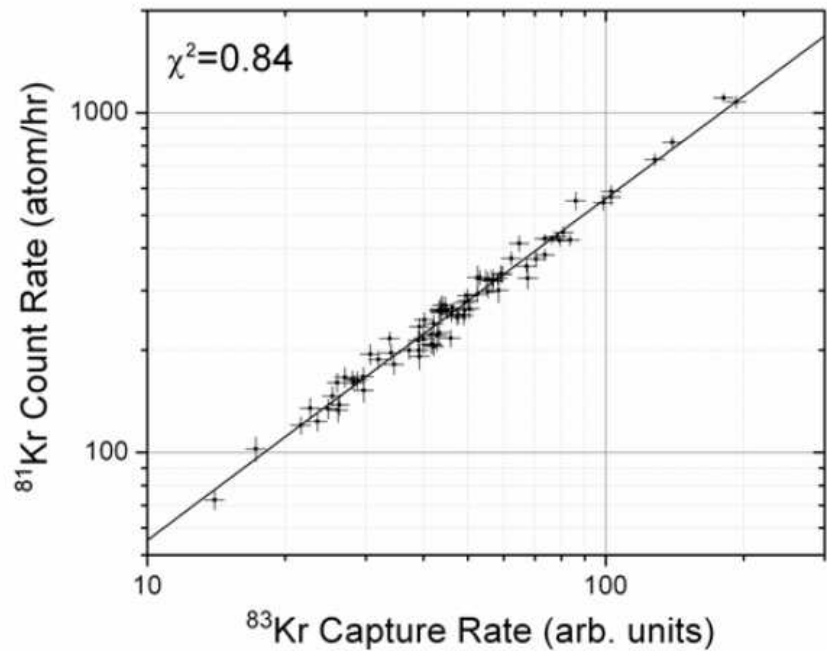


FIG. 4. (a)  $^{39}\text{Ar}$  atom counts as a function of laser frequency. Atoms were detected only at a laser frequency of  $-6$  MHz relative to the cycling transition. The dashed line represents the normalized loading rate of  $^{81}\text{Kr}$  on the same relative frequency scale for comparison. (b)  $^{39}\text{Ar}$  counts per 60 hours at  $-6$  MHz for the atmospheric and depleted sample.

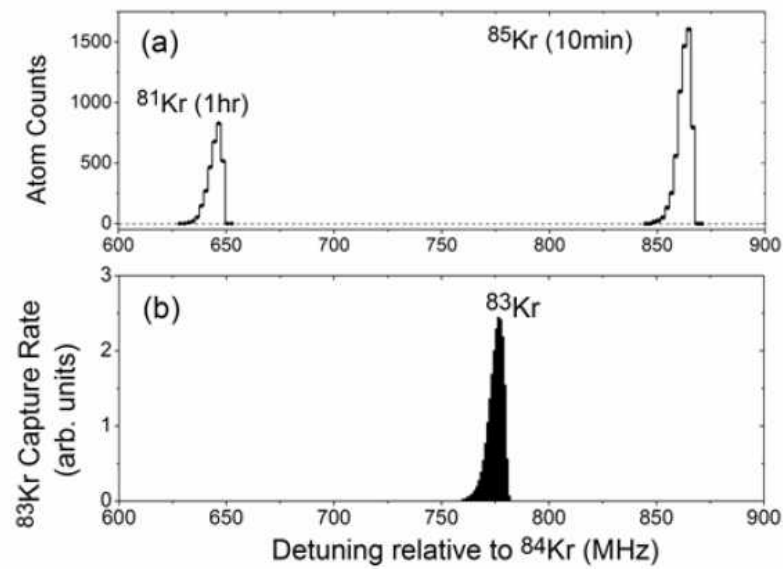
PRL 106, 103001 (2011)

*Long lived isotopes are also good for dating, but the longer the life time the harder they are to radiologically count.*



Argonne National lab has been able to ratio Krypton isotopes in order to accurately date water supplies.

Rapid detection of isotopes is possible regardless of their half life. Kr-85 (10.7yrs) Kr-81( $2 \times 10^{10}$  yrs) Kr-83 is stable



<http://dx.doi.org/10.1016/j.gca.2012.05.019>

All the atoms that have been laser cooled, trapped, and measured

**PERIODIC TABLE OF THE ELEMENTS**

<http://www.ktf-split.hr/periodni/en/>

PERIOD

GROUP

1 1.0079 H HYDROGEN 2 9.0122 Be BERYLLIUM 3 6.941 Li LITHIUM 11 22.990 Be BORON 13 10.811 BORON

2 12.4305

3 26.982 Al ALUMINUM 14 28.086 Si SILICON 15 30.974 P PHOSPHORUS 16 32.065 S SULPHUR 17 35.453 Cl CHLORINE 18 39.948 Ar ARGON

4 19.998 O OXYGEN 8 15.999 F FLUORINE 9 18.998 Ne NEON 10 20.180

5 39.098 K POTASSIUM 19 40.078 Ca CALCIUM 20 44.956 Sc SCANDIUM 21 47.867 Ti TITANIUM 22 50.942 V VANADIUM 23 51.996 Cr CHROMIUM 24 54.938 Mn MANGANESE 25 55.845 Fe IRON 26 58.933 Co COBALT 27 58.693 Ni NICKEL 28 63.546 Cu COPPER 29 65.39 Zn ZINC 30 69.723 Ga GALLIUM 31 72.64 Ge GERMANIUM 32 74.922 As ARSENIC 33 78.96 Se SELENIUM 34 79.904 Br BROMINE 35 83.80 Kr KRYPTON

6 37 85.468 Rb RUBIDIUM 38 87.62 Sr STRONTIUM 39 88.906 Y YTTRIUM 40 91.224 Zr ZIRCONIUM 41 92.906 Nb NIOBIUM 42 95.94 Mo MOLYBDENUM 43 (98) Tc TECHNETIUM 44 101.07 Ru RUTHENIUM 45 102.91 Rh RHODIUM 46 106.42 Pd PALLADIUM 47 107.87 Ag SILVER 48 112.41 Cd CADMIUM 49 114.82 In INDIUM 50 118.71 Sn TIN 51 121.76 Sb ANTIMONY 52 127.60 Te TELLURIUM 53 126.90 I IODINE 54 131.29 Xe XENON

7 55 132.91 Cs CAESIUM 56 137.33 Ba BARIUM 57-71 La-Lu Lanthanide 57-71 Hf HAFNIUM 58 Ta TANTALUM 59 W TUNGSTEN 60 Re RHENIUM 61 Os OSMIUM 62 Ir IRIDIUM 63 Pt PLATINUM 64 Au GOLD 65 Hg MERCURY 66 Tl THALLIUM 67 Pb LEAD 68 Bi BISMUTH 69 Po POLONIUM 70 At ASTATINE 71 Rn RADON

LANTHANIDE

57 138.91 La LANTHANUM 58 140.12 Ce CERIUM 59 140.91 Pr PRASEODYMIUM 60 144.24 Nd NEODYMIUM 61 (145) Pm PROMETHIUM 62 150.36 Sm SAMARIUM 63 151.96 Eu EUROPIUM 64 157.25 Gd GADOLINIUM 65 158.93 Tb TERBIUM 66 162.50 Dy DYSPROSIDIUM 67 164.93 Ho HOLMIUM 68 167.26 Er ERBIUM 69 168.93 Tm THULIUM 70 173.04 Yb YTTERBIUM 71 174.97 Lu LUTETIUM

ACTINIDE

89 (227) Ac ACTINIUM 90 232.04 Th PROTACTINIUM 91 231.04 Pa URANIUM 92 238.03 U NEPTUNIUM 93 (237) Np NEPTUNIUM 94 (244) Pu PLUTONIUM 95 (243) Am AMERICIUM 96 (247) Cm CURIUM 97 (247) Bk BERKELIUM 98 (251) Cf CALIFORNIUM 99 (252) Es EINSTEINIUM 100 (257) Fm FERMUM 101 (258) Md MENDELEIUM 102 (259) No NOBELIUM 103 (262) Lr LAWRENCIUM

(1) Pure Appl. Chem., 73, No. 4, 667-683 (2001)  
Relative atomic mass is shown with five significant figures. For elements have no stable nuclides, the value enclosed in brackets indicates the mass number of the longest-lived isotope of the element.  
However three such elements (Th, Pa, and U) do have a characteristic terrestrial isotopic composition, and for these an atomic weight is tabulated.

Editor: Aditya Vardhan (adivar@netlinx.com)

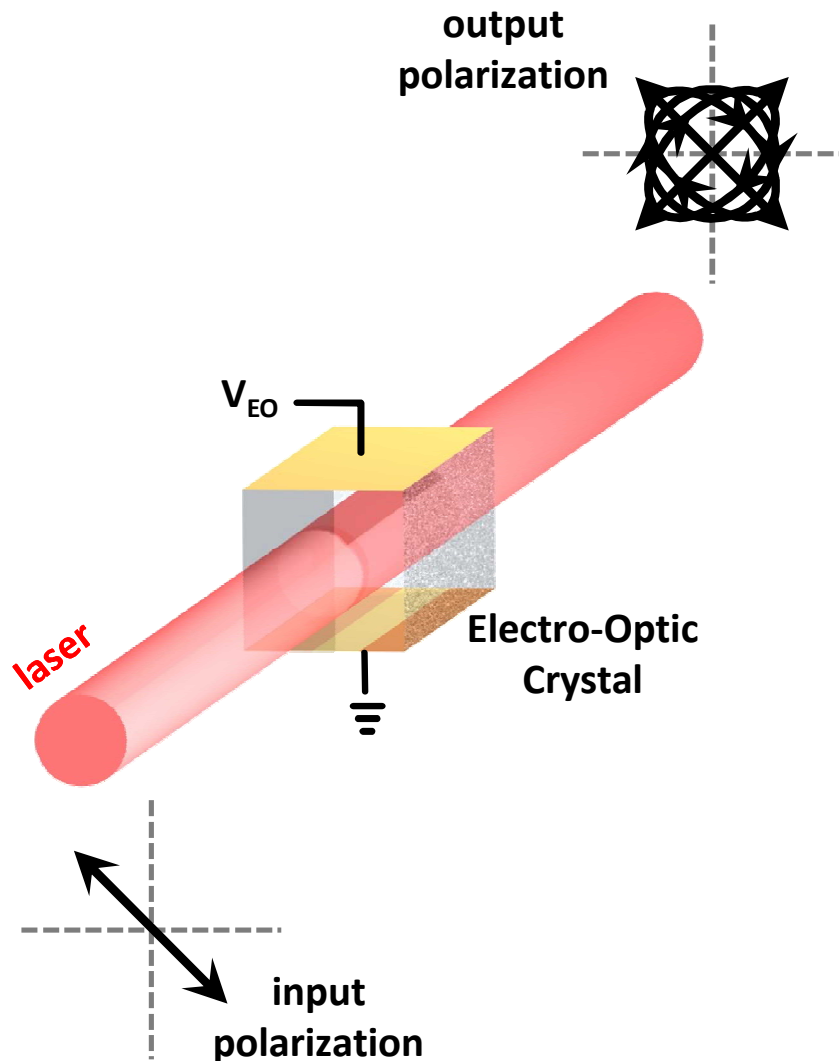
Copyright © 1998-2003 EniG (eni@ktf-split.hr)

*New detector techniques: can we use lasers to detect radiological decay?*



- Standard radiation detectors have been identified as having shortfalls.
- Signal size (i.e. number of photons or electrons detected) is directly proportional to the energy and type of the incoming particle

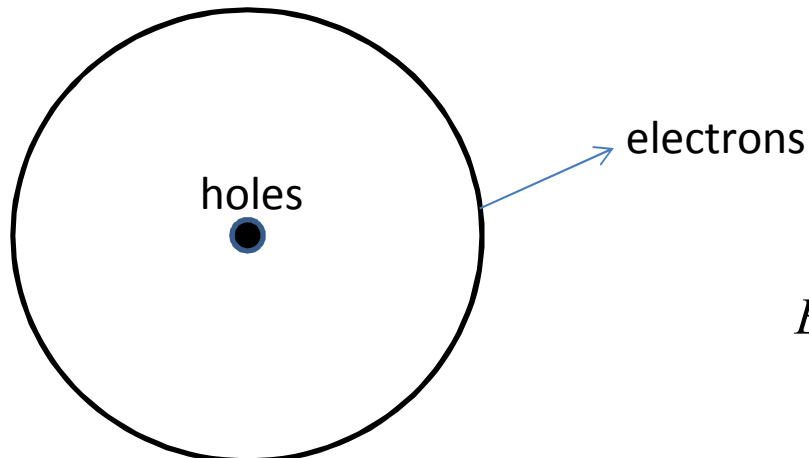
**Can we produce a detector whose signal size is independent of the energy deposited in the detector?**

*Laser amplified particle detector.*

- Commercially available crystals include KDP, ADP,  $\text{LiNbO}_3$ ,  $\text{LiTaO}_3$
- Pockels effect- production of birefringence in a noncentrosymmetric crystal that is proportional to the applied electric field
- Applied electric field creates a change in index of refraction,  $\Delta n$

*Hole pair migration*

- Theoretical models indicate an external electric field is needed for significant changes in index of refraction
- External field model assumes
  - Holes are immobile
  - Electric field will separate the electrons from the holes
  - Electrons form a thin cylindrical shell as they drift



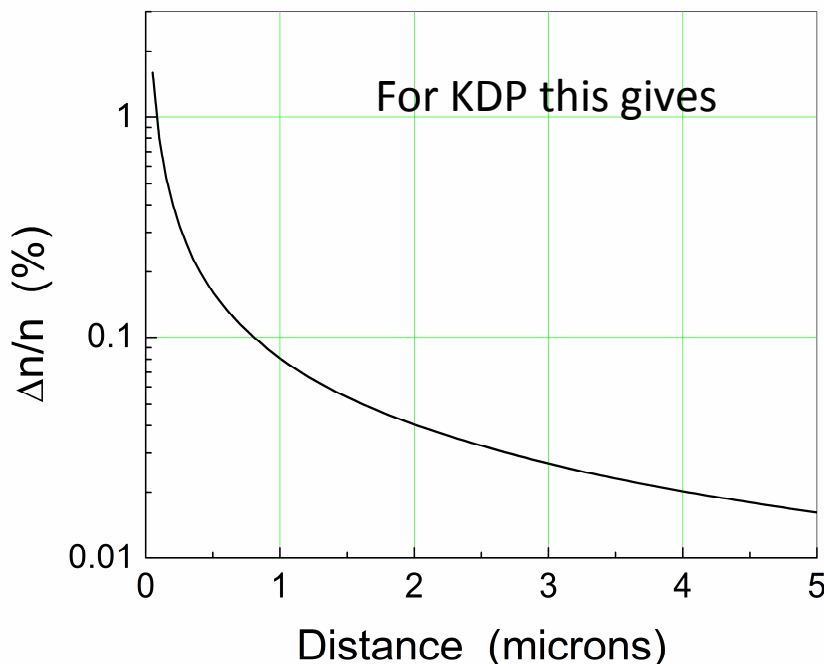
The electric field is easy to calculate:

$$E(r) = \begin{cases} -\frac{\rho}{2\pi\epsilon r} & \text{inside the electron cylinder} \\ 0 & \text{outside the electron cylinder} \end{cases}$$

- So the external electric field essentially serves the purpose of giving the intrinsic electric field of the isolated hole distribution, up to the separation distance between electrons and holes.

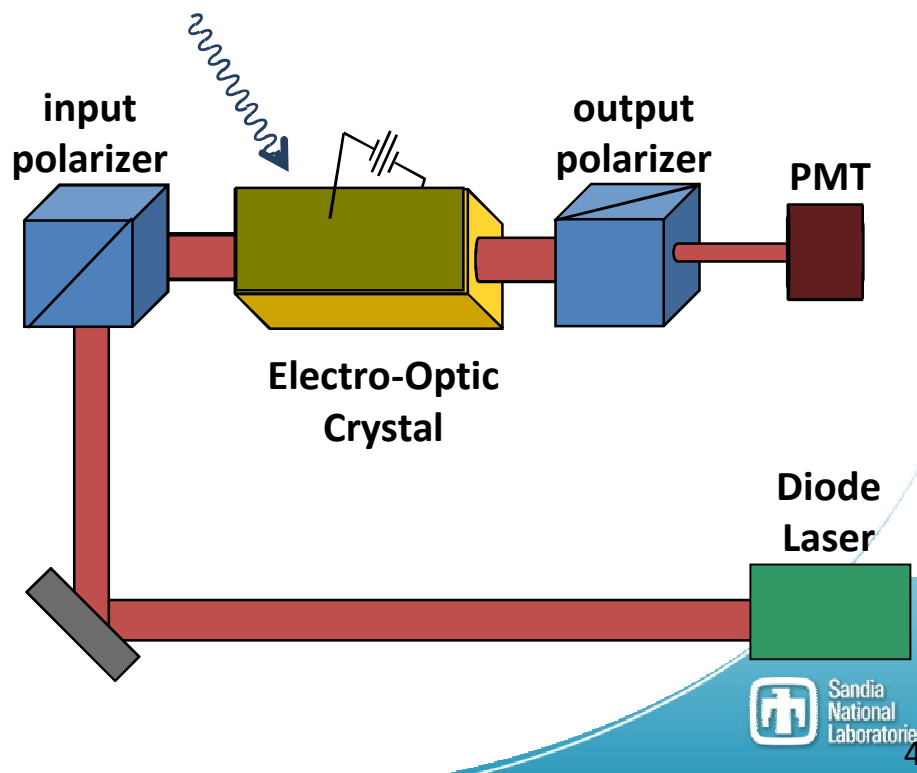
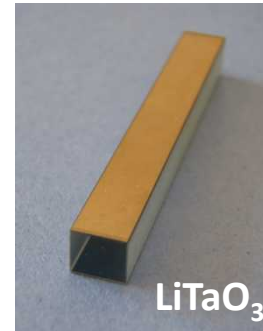
**The electro-optic effect as a function of distance from the hole line would be:**

$$\frac{\Delta n}{n} = \frac{n^2 r_{eo} \rho}{4\pi\epsilon r}$$

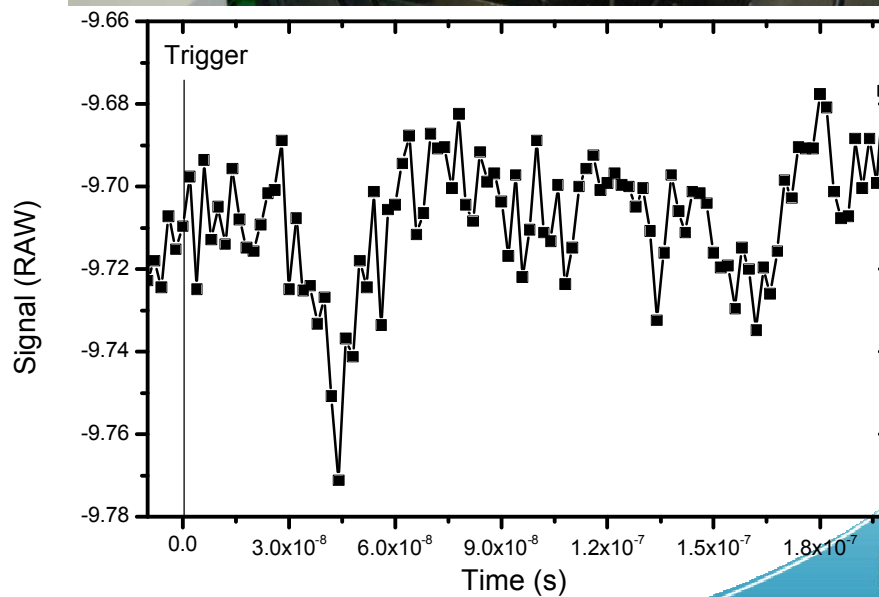
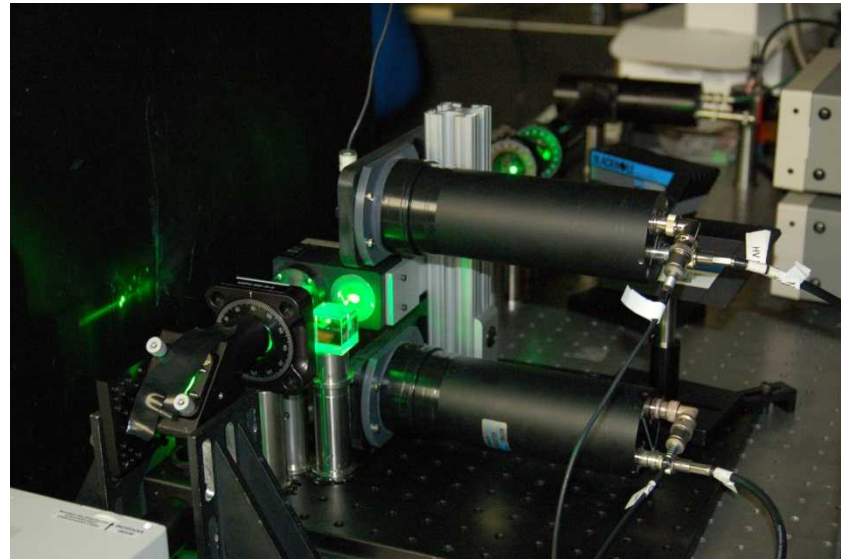
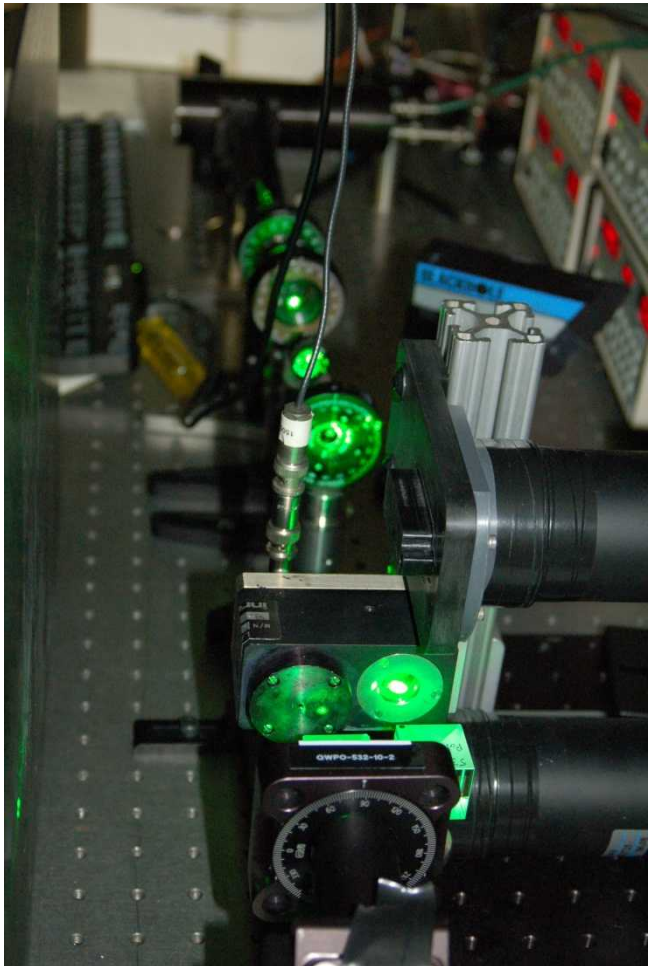


## *Experimental setup*

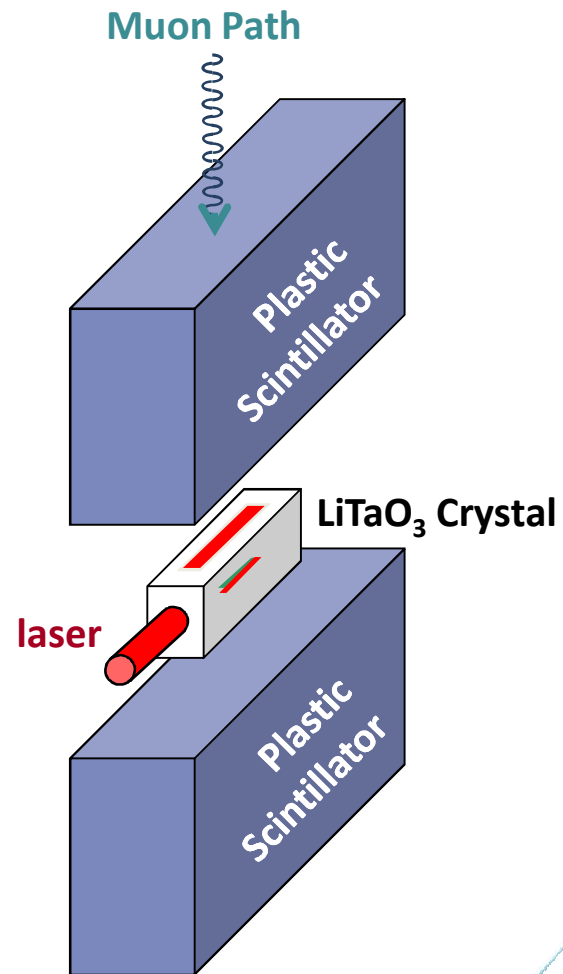
- Electro-optic crystals:
  - 15 x 15 x 25 mm KDP (commercial Q switch)
  - 5×5×20 mm LiTaO<sub>3</sub> with gold electrodes
- Applied voltages: (±)0.7 – 3 kV
- Lasers:
  - cw, 780 nm, 10 mW
  - cw 532 nm, 5 W
- Detector: PMT w/AC amplifier
- Temporally-resolved, spatially-integrated signal recorded on an oscilloscope
- Uses polarization spectroscopy

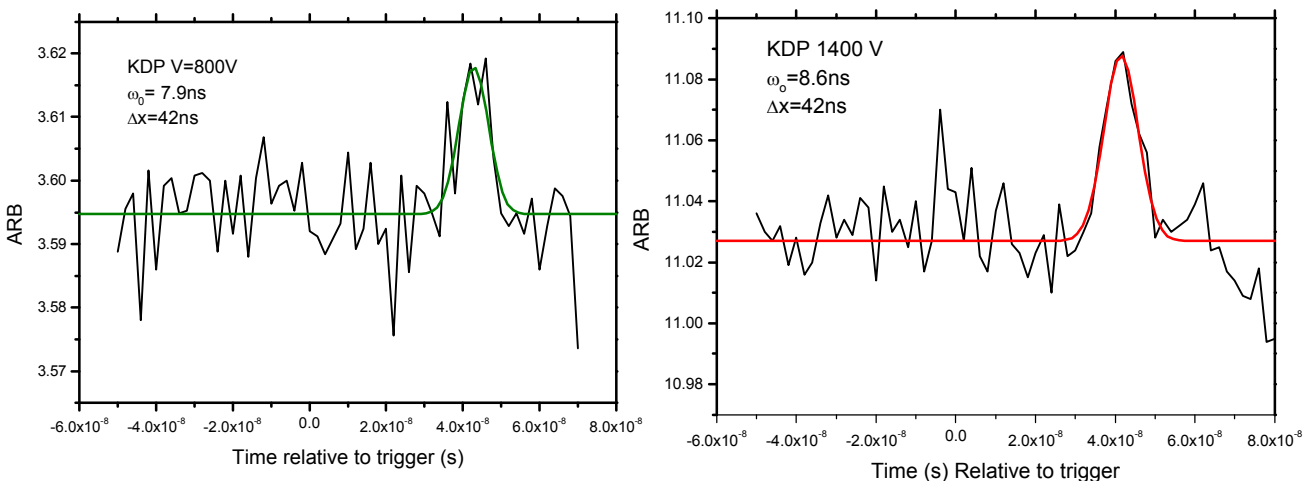


*The proof of principle*



- Muon interaction with  $\text{LiTaO}_3$ :
  - 4 MeV/cm deposited within the  $\text{LiTaO}_3$  crystal with 4-eV band gap
  - 150,000 electron-hole pairs created due to radiation interaction
  - Linear electron-hole pair density:  $30/\mu\text{m}$
- Collection of signal corresponding to interaction of muon with the crystal requires knowledge of muon occurrence
- Trigger signal collection with response from pair of plastic scintillators
  - Trigger requires high light levels on both upper and lower scintillator
  - Observed trigger rate:  $\sim 3 \text{ mHz}$ , or 1 every 6 min





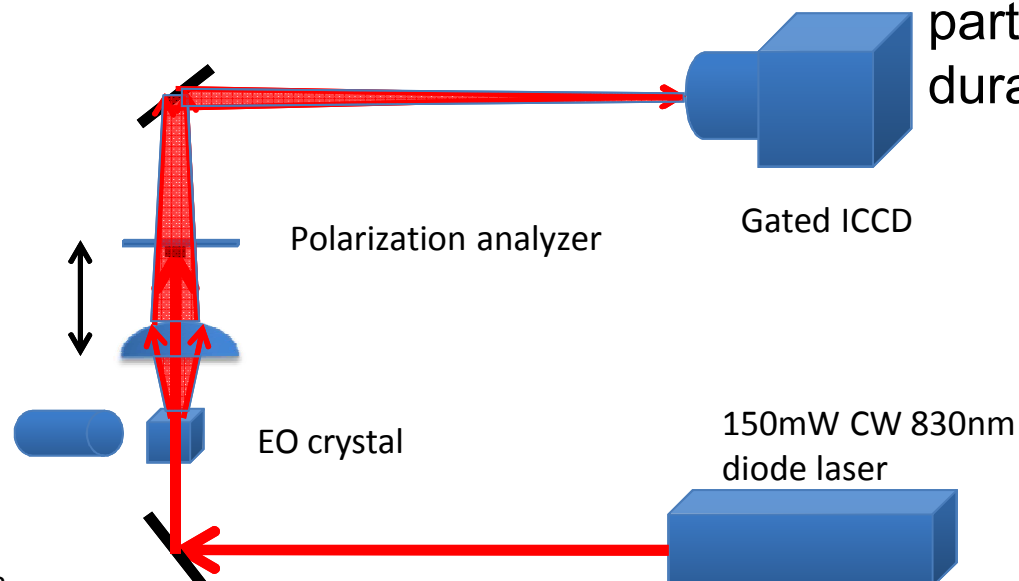
KDP 2200 V  
 $w_0 = 14\text{ ns}$

- Average of 130 triggers
- 0.5 % of the light on the tracks is rotated to pass through the cross polarizer
- 0.75 ns / 100 V change in the track duration
- Significant reduction in noise due to polarization impurity
  - Replaced mirrors with metal coatings
  - True 45° light reflections
  - Limited by electronic noise

*Imaging*

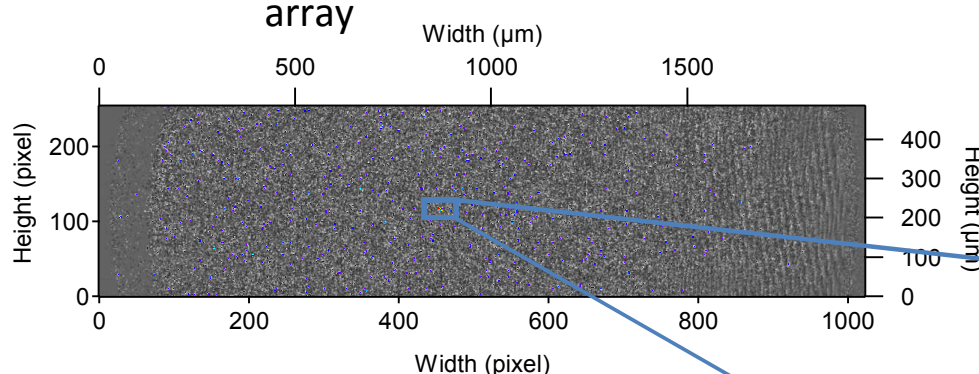
Pros	Cons
------	------

- Allows for larger signal to noise
- Allows for spatially reconstruction of the particle  $dE/dx$
- Allows for the direct imaging of electron-hole recombination



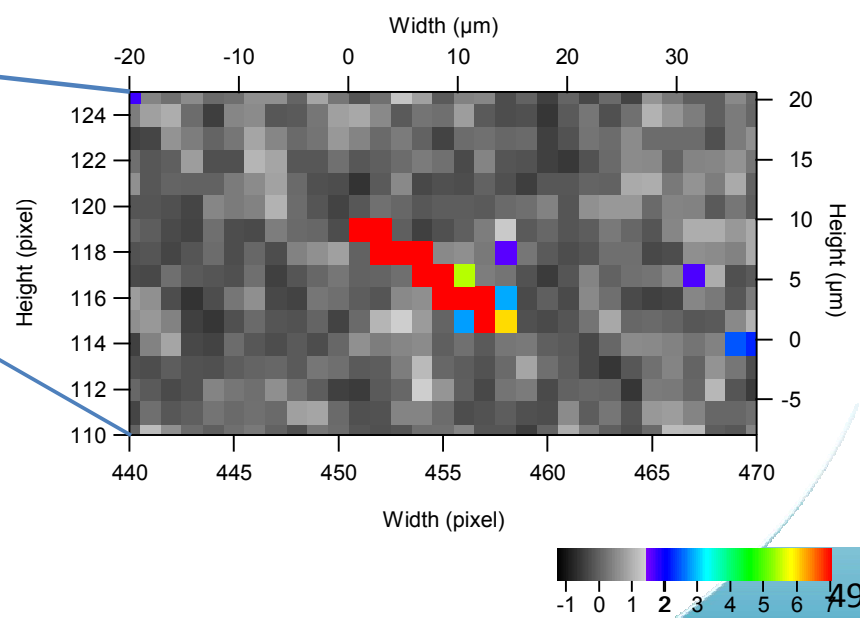
- **Fast Neutron Imaging**

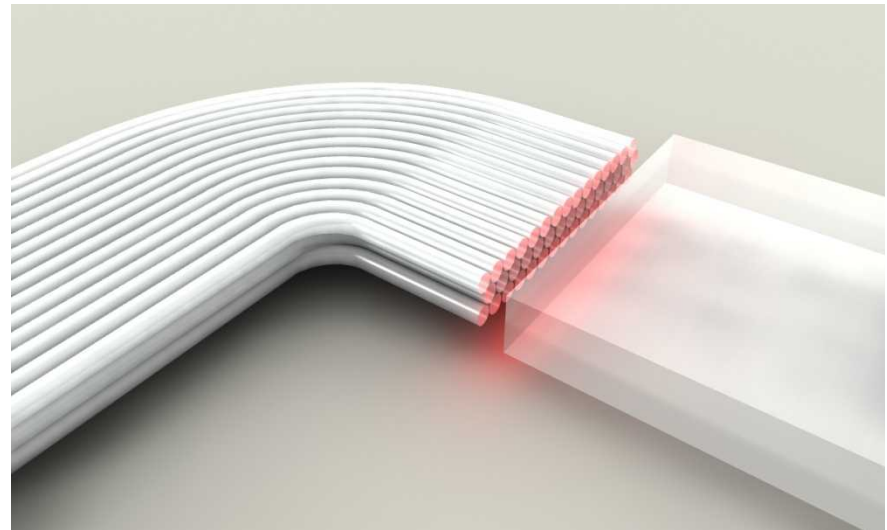
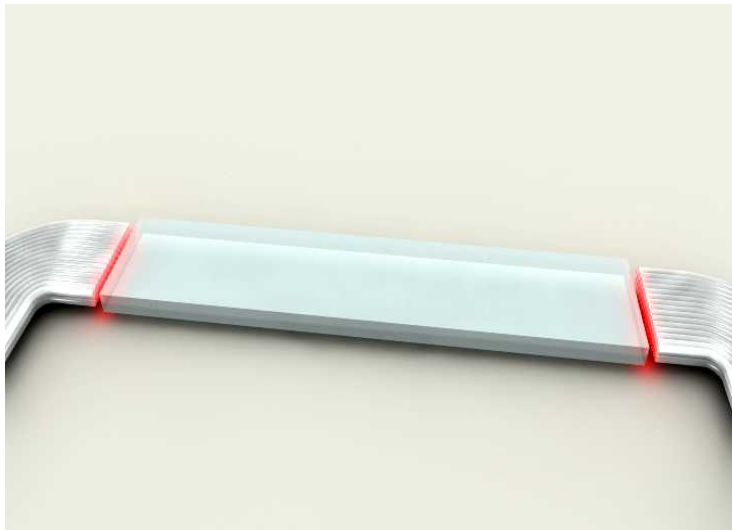
- High flux  $\sim 10^7$  neutrons/10 $\mu$ s
- D-T neutrons  $\sim 14$  MeV
- Triggerable
- Integrated with gated intensified CCD array



- **Size: ~9 pixels (~18  $\mu$ m) long**
- **Width: 8 pixels**
- **Intensity: multiple pixels  
>50x background**

- Neutral Particle interactions are probabilistic, not deterministic
- Limited depth of field for imaging implies 1 image/100 minutes





- Signal strength is dependent on a user adjustable external probe laser
- Reduced power consumption of the installed detector components
- Reduction in the support infrastructure including a wireless readout system
- Quick recovery time  $\sim 8$  ns of the material after particle interaction
- Radiation-hard material that can be placed close to the collision region.
- Ability to operate in large magnetic fields

